Deutsches Zentrum
für Luft- und Raumfahrt e.V.
in der Helmholtz-Gemeinschaft

EnMAP Ground Segment

Mission Quarterly Report #02

01.10.2022 to 31.12.2022

Restriction: public

Doc. ID	EN-GS-RPT-1102
Issue	1.0
Date	21.03.2023

Configuration Controlled: Yes

German Remote Sensing Data Center (DFD)
Remote Sensing Technology Institute (IMF)
German Space Operations Center (GSOC)
German Research Centre for Geosciences (GFZ-Potsdam)
German Space Agency at DLR

TABLE OF SIGNATURES

Prepared

Tobias Storch
Digital signiert von Tobias Storch
DN: C=DE, OU=MF-PBA, O=DLR, CN=Tobias Storch, E=tobias.storch@dlr.de
Grund:
Ort:
Datum: 2023.04.21 12:32:35+02'00'
Foxit PDF Editor Version: 12.1.1

Date Tobias Storch, (DLR MF-PBA, EnMAP OMM)

Sabine Chabrillat
Digital unterschrieben von Sabine Chabrillat
Datum: 2023.04.25 13:41:24 +02'00'

Date Sabine Chabrillat, (GFZ-Potsdam, EnMAP SciLead)

Reviewed

K. Wirth
Katrin Wirth
2023.04.28 07:43:41+02'00'

Date Katrin Wirth, (DLR RB-MIB, dep. EnMAP OMM)

Sabine Engelbrecht
Digital signiert von Sabine Engelbrecht
DN: C=DE, S=Nordrhein-Westfalen, L=Koeln, O=Deutsches Zentrum fuer Luft- und Raumfahrt e.V. (DLR), SN=Engelbrecht, G=Sabine, CN=Sabine Engelbrecht
Grund: Ich habe dieses Dokument geprüft
Ort: Oberpfaffenhofen
Datum: 2023.05.02 15:01:14+02'00'
Foxit PDF Editor Version: 12.1.1

Date Sabine Engelbrecht, (DLR DFD-INF, EOC PAD)

Digital signiert von Johannes Greulich
Datum: 2023.05.02 15:11:26+02'00'

Date Johannes Greulich, (DLR RB-MIB, GSOC PAD)

Karl Segl
Digital unterschrieben von Karl Segl
Datum: 2023.04.22 06:53:24 +02'00'

Date Karl Segl, (GFZ-Potsdam, dep. EnMAP SciLead)

Approved & Released

i.A. S. Fischer
Digital signiert von Sebastian Fischer
Datum: 2023.05.17 15:33:28 +02'00'

Date Sebastian Fischer, (DLR AR-AO, EnMAP MM)

DISTRIBUTION LIST

The document is publicly available via www.enmap.org.

CHANGE RECORD

Version	Date	Chapter	Comment
1.0	21.03.2022	All	First issue of Mission Quarterly Report #02

Custodian of this document is Storch, Tobias.

CONTENTS

LIST OF FIGURES

LIST OF TABLES

1. Introduction

1.1 Purpose

This mission quarterly report (MQR) states information on the EnMAP mission status with regard to the registered user community, announcements-of-opportunities and observations as well as the status of the user interfaces, satellite (platform and payload), ground stations (S-band and X-band), processor (Archive, Level 1B, Level 1C, Level 2A (land and water)), calibration (spectral, radiometric, geometric), data quality control and validation of EnMAP.

Please visit www.enmap.org for further information on EnMAP.

1.2 Scope

This second Mission Quarterly Report (MQR) applies to the operations of EnMAP in the #02 reporting period from **01.10.2022 to 31.12.2022 (Q4/2022)**. It refers to the Commissioning Phase (CP) of EnMAP, i.e. 01.10.2022 to 01.11.2022 and the Routine Phase (RP) of EnMAP, i.e. 02.11.2022 to 31.12.2022.

2. References

Reference Identifier	Document Identifier and Title
[1]	L. Guanter et al. (2015) The EnMAP Spaceborne Imaging Spectroscopy Mission for Earth Observation. Remote Sensing, Issue 7, pp. 8830-8857.
[2]	EN-GS-UM-6020 Portals User Manual, Version 1.0
[3]	EN-PCV-ICD-2009 Product Specification, Version 1.8
[4]	EN-PCV-TN-4006 Level 1B ATBD, Version 1.7
[5]	EN-PCV-TN-5006 Level 1C ATBD, Version 1.6
[6]	EN-PCV-TN-6007 Level 2A (land) ATBD, Version 2.2
[7]	EN-PCV-TN-6008 Level 2A (water) ATBD, Version 3.1
[8]	Chabrillat, S. et al. (2022) EnMAP Science Plan. EnMAP Technical Report, DOI: 10.48440/enmap.2022.001
[9]	Lachérade, S. et al. (2014) Introduction to the Sentinel-2 radiometric calibration activities during commissioning phase. Proc. SPIE, Vol. 9241, DOI: 10.1117/12.2067123

Table 2-1: References

3. Terms, Definitions and Abbreviations

Terms, definitions and abbreviations for EnMAP are collected in a database which is publicly accessible via Internet on www.enmap.org.

An Earth observation of swath length $n \times 30$ km (and swath width 30 km) is separated into n tiles of size 30 km × 30 km.

4. Mission

4.1 Mission Objectives

The primary goal of EnMAP (Environmental Mapping and Analysis Program) is to measure, derive and analyze quantitative diagnostic parameters describing key processes on the Earth's surface [1].

During the mission operations, with the successful launch on 1st of April 2022 and an expected operational mission lifetime of at least 5 years, EnMAP will provide valuable information for various application fields comprising soil and geology, agriculture, forestry, urban areas, aquatic systems, ecosystem transitions.

4.2 Mission Description

The major elements of the EnMAP mission are the EnMAP Space Segment, built by OHB System AG and owned by the German Space Agency at DLR, the EnMAP Ground Segment built and operated by DLR institutes DFD, MF, RB, and the EnMAP User and Science Segment represented by GFZ. The project management of the EnMAP mission is responsibility of the German Space Agency at DLR.

The EnMAP Space Segment is composed of

- the platform providing power and thermal stability, orbit and attitude control, memory, S-band uplink/downlink for TM/TC data transmission/reception, X-band downlink for payload data transmission, and
- the payload realized as a pushbroom imaging dual-spectrometer covering the wavelength range between 420 nm and 2450 nm with a nominal spectral resolution ≤ 10 nm and allows in combination with a high radiometric resolution and stability to measure subtle reflectance changes.

The EnMAP satellite is operated on a sun-synchronous repeat orbit to observe any location on the globe with comparable illumination conditions. This allows a maximum reflected solar input radiance at the sensor with an acceptable risk for cloud coverage.

The EnMAP Ground Segment is the interface between Space Segment and User and Science Segment. It comprises functionalities to

- perform planning of imaging, communication and orbit maneuver operations, provision of orbit and attitude data, command and control of the satellite, ground station networks (in particular: Weilheim, Germany, for S-band and Neustrelitz, Germany, for X-Band), receive satellite data, perform long-term archiving and delivery of products, and
- perform processing chain (for systematic and radiometric correction, orthorectification, atmospheric compensation), instrument calibration operations, and the data quality control of the products.

The EnMAP mission interfaces to the international science and user community through the EnMAP Portal www.enmap.org with official information related to EnMAP by DLR and GFZ-Potsdam (as the document in hand) and links for ordering observations and products.

The EnMAP Science Segment is represented by the EnMAP Science Advisory Group chaired by the mission principal investigator at the GFZ-Potsdam. The Science Segment addresses aspects such as

- supporting and performing validation activities to improve sensor performance and product quality
- developing scientific and application research to fully exploit the scientific potential of EnMAP [8] including provision of software tools for EnMAP data processing and analyses (EnMAP-Box) and provision of teaching and education materials (HYPERedu)
- Organizing workshops, summer schools and in general information, training and networking activities for the user community

The EnMAP User Segment is the community of German and international users ordering acquisitions and accessing products of EnMAP.

4.3 Mission Status Summary

The mission was in its commissioning phase (CP; 01.10.2022-28.10.2022, successfully finished as planned) and is in its routine phase (RP, since 02.11.2022).

On 13.12.2022 an instrument anomaly occurred and Earth observations and Calibrations are not performed. Intense tests were required in December 2022. In January 2023 the instrument software was patched. In February 2023 tests and instrument data checks were performed. On 13.02.2023 the instrument anomaly was recovered, where no limitations of functionality persist and no use of redundancies required.

962 Earth observations of 30 km swath width and up to 990 km swath length were successfully performed between 01.10.2022 and 12.12.2022 which resulted in 6,208 archived Earth observation tiles of 30 km × 30 km. In total, 2,802 Earth observations were performed until 31.12.2022 by the 221 registered users which resulted in 16,998 archived Earth observation tiles and 17,534 Earth observation tiles were delivered to users. Details are presented in Sections 5 and 6.

The following limitations are applicable at 31.12.2022:

- Instrument Anomaly (see above)
- Continuous degradation of the VNIR sensor of 20.06.2022: 0.06%/day was observed and addressed during commissioning phase by more frequent adjustments of the radiometric calibration. However, the rate of degradation has been decreasing to 30.09.2022: 0.03%/day and is expected to reach a negligible magnitude in March 2023. If this is the case, radiometric requirements are expected to remain within specifications.
- Some striping effects are visible in VNIR and SWIR data, in particular for low radiances. However, the radiometric requirements of the mission are met.
- Limitations on user interfaces apply as detailed in section 7.1 and are considered in [2].

The following changes are expected to be performed until 31.03.2023 and later:

- Recovery of Instrument Anomaly (see above)
- Limitations on user interfaces are expected to be solved by the end of Q1/2023 respectively during Q2/2023 as detailed in section 7.1.
- To avoid leaps in consecutive radiometric calibration coefficients, due to the degradation of the VNIR sensor, modifications in the radiometric calibration and radiometric correction processor are expected by early 2023.
- Further improvements to the radiometric correction processor, e.g. for mitigating the striping effects, are expected to be realized by early 2023.
- Further improvements of the archive, e.g. on quicklooks and quality attributes, are expected by a re-processing planned by early 2023. The quality of delivered products will not be affected, because therefore, the current processors are used anyway.

5. Users and Announcements-of-Opportunities

5.1 Users

Category	Country/*Continent (No of Countries)*	02.11.2022 to 31.12.2022
Cat-1 Science and Catalogue User	Total	715
	Europe (27)	442
	• Germany	228
	• Italy	38
	• France	25
	• Great Britain	26

Category	Country/*Continent (No of Countries)*	02.11.2022 to 31.12.2022
	• Espania	24
	• Netherlands	13
	• Portugal	12
	• Turkey	14
	• Others	62
	North America (2)	79
	South America (8)	49
	Asia (13)	81
	Africa (16)	41
	Australia + New Zealand (2)	23
Rejected	Total	1

Table 5-1 Number of registered users per continent.

Users are rejected because of, e.g. EU sanction list checks, data policy or license violations.

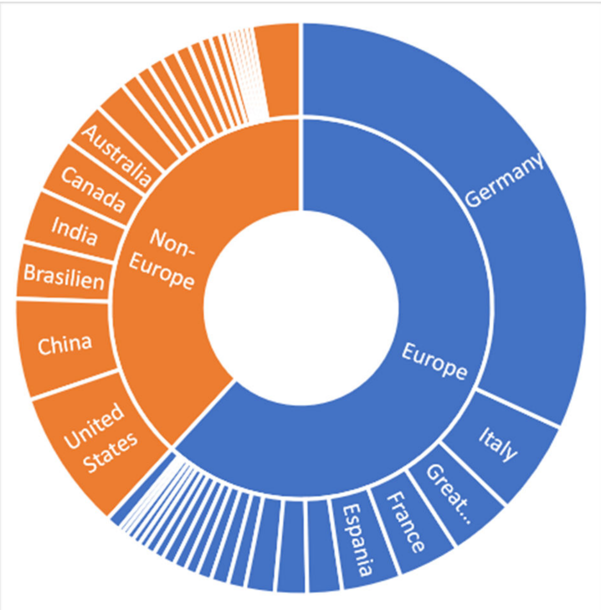

02.11.2022 to 31.12.2022 with total of 715 users of 69 different countries worldwide

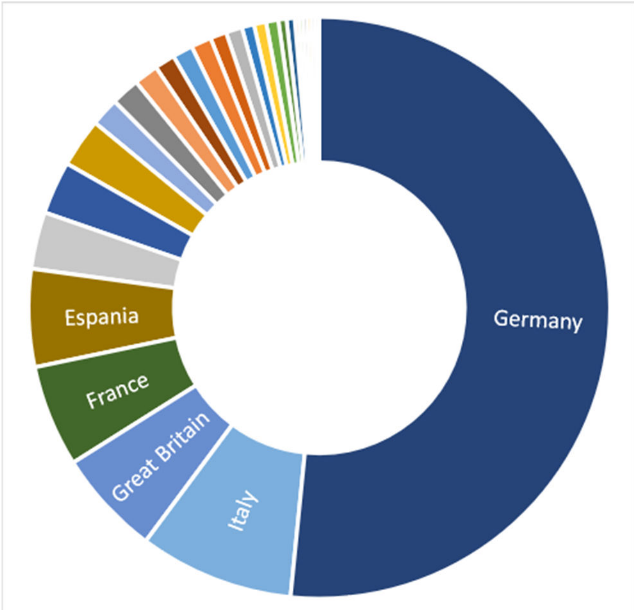

02.11.2022 to 31.12.2022 with total of 442 European users of 27 countries

Figure 5-1 Number of registered users

Registered users belong to different categories, therefore e.g. All/World ≠ Science/World + Others/World.

5.2 Announcements-of-Opportunities

Announcement-of-Opportunity	Decision	02.11.2022 to 31.12.2022	
		Proposals	Total Tiles
AO#1	Accepted	31	2774
	Rejected	1	140
AO#2	Accepted	19	2288
	Rejected	0	0
Total	Accepted	50	5062
	Rejected	1	140

Table 5-2 Number of science proposals to Announcement-of-Opportunity

Icon	Topic	02.11.2022 to 31.12.2022	
		Proposals	Total Tiles
	VEGETATION	18	2207
	GEO/SOIL	14	442
	WATER	9	868
	SNOW/ICE	0	0
	URBAN	0	0
	ATMOSPHERE	2	385
	HAZARD/RISK	0	0
	METHODS	1	120
	CAL/VAL	6	1040
	Total	50	4090

Table 5-3 Number of accepted science proposals to Topic

6. Archived and Delivered Observations

The following table shows the number of archived Earth Observation and Calibration products and their sizes within the specified time frames.

Type	Archived		01.10.2022 to 31.12.2022		until 31.12.2022	
			Number Tiles / Observations	Size (in GB)	Number Tiles / Observations	Size (in GB)
Earth Observation (EO)	Yes	Total	6208 / 962	2895.4	16998 / 2802	7930.9
		Average / Day	67.5 / 10.5	31.5	61.8 / 10.2	28.8
	No	Total	443		559	
		Average / Day	4.8		2.0	
Calibration (CAL)	Yes	Total	20	85.0	71	313.1
		Average / Day	0.2	0.9	0.3	1.1
	No	Total	0		1	
		Average / Day	0		0.004	

Table 6-1 Number and size of archived and not archived products

The following table shows the number of delivered products and their sizes within the specified time frames. Product deliveries result either directly from acquisition orders (Observation) and catalog orders (Archive)

Type	Delivered		01.10.2022 to 31.12.2022		until 31.12.2022	
			Number Tiles / Observations	Size (in GB)	Number Tiles / Observations	Size (in GB)
Earth Observation (EO)	Observation	Total	8623 / 1068	3741.7	17534 / 2484	7654.0
		Average / Day	93.7 / 11.6	40.7	64.9 / 9.0	27.8
	Archive	Total	2903	12722.7	4810	23473.9
		Average / Day	31.6	138.3	17.5	85.4
Calibration (CAL)	Observation	Total	17	79.1	50	242.2
		Average / Day	0.2	0.9	0.2	0.9
	Archive	Total	60	3058.7	67	3091.1
		Average / Day	0.7	33.2	0.2	11.2

Table 6-2 Number and size of delivered products

6.1 Archived Observations

The following figures show the heatmaps for the whole world and for Europe within the specified time frames. The heatmaps represent the frequencies of products at a geographic location, where the number of products increases from blue over red to yellow.

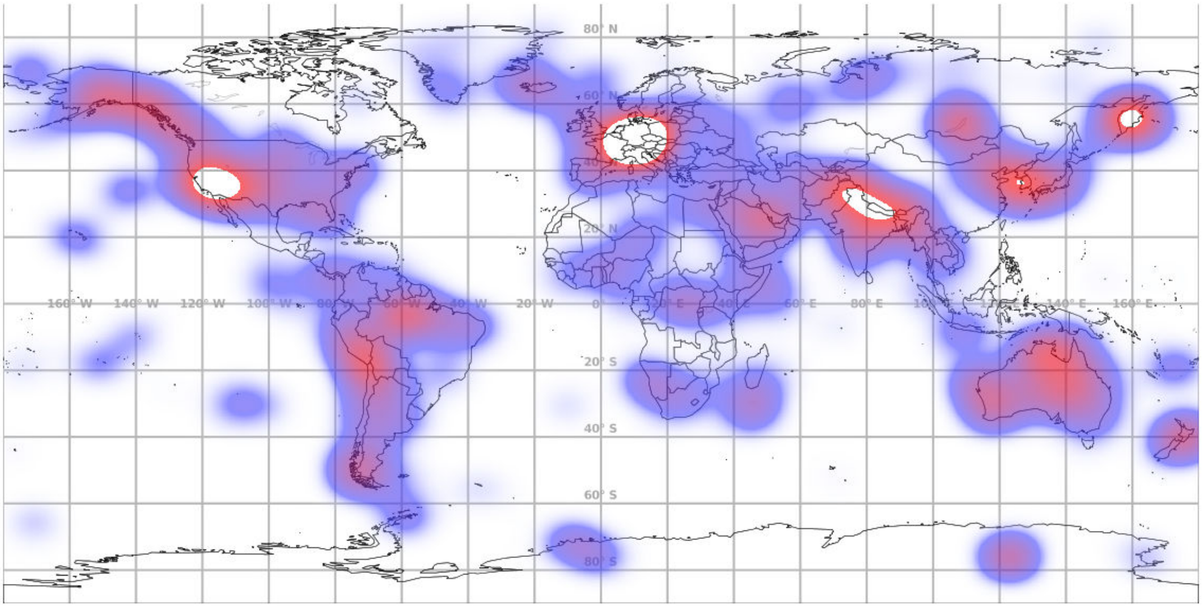

01.10.2022 to 31.12.2022 with 6208 tiles

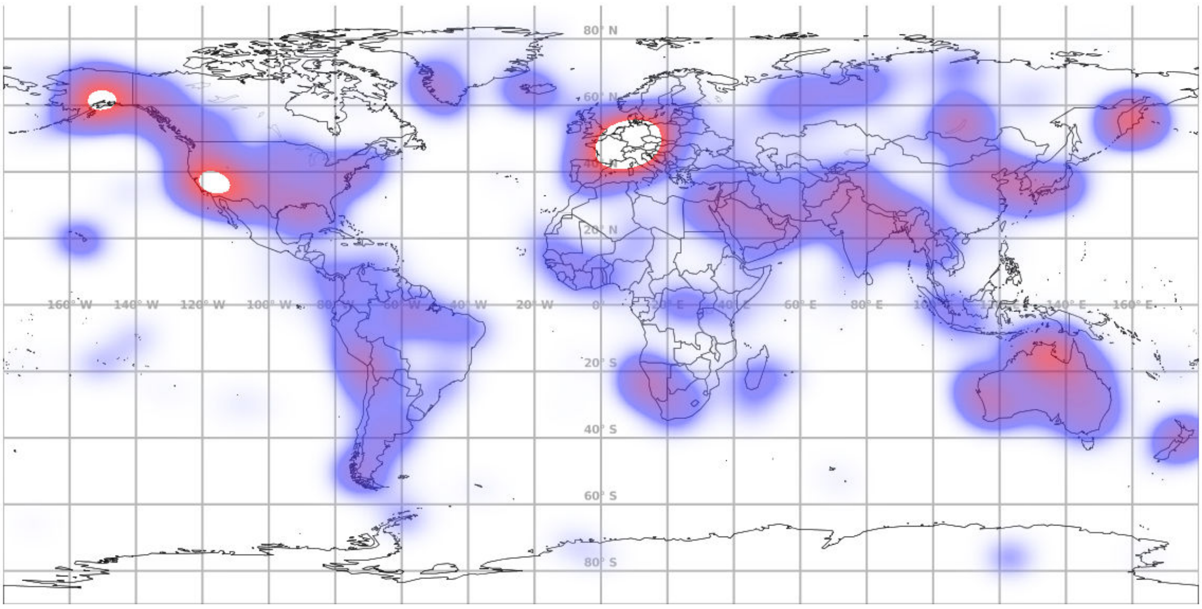

until 31.12.2022 with 17534 tiles

Figure 6-1 Geographic location of all Earth observation tiles archived, World

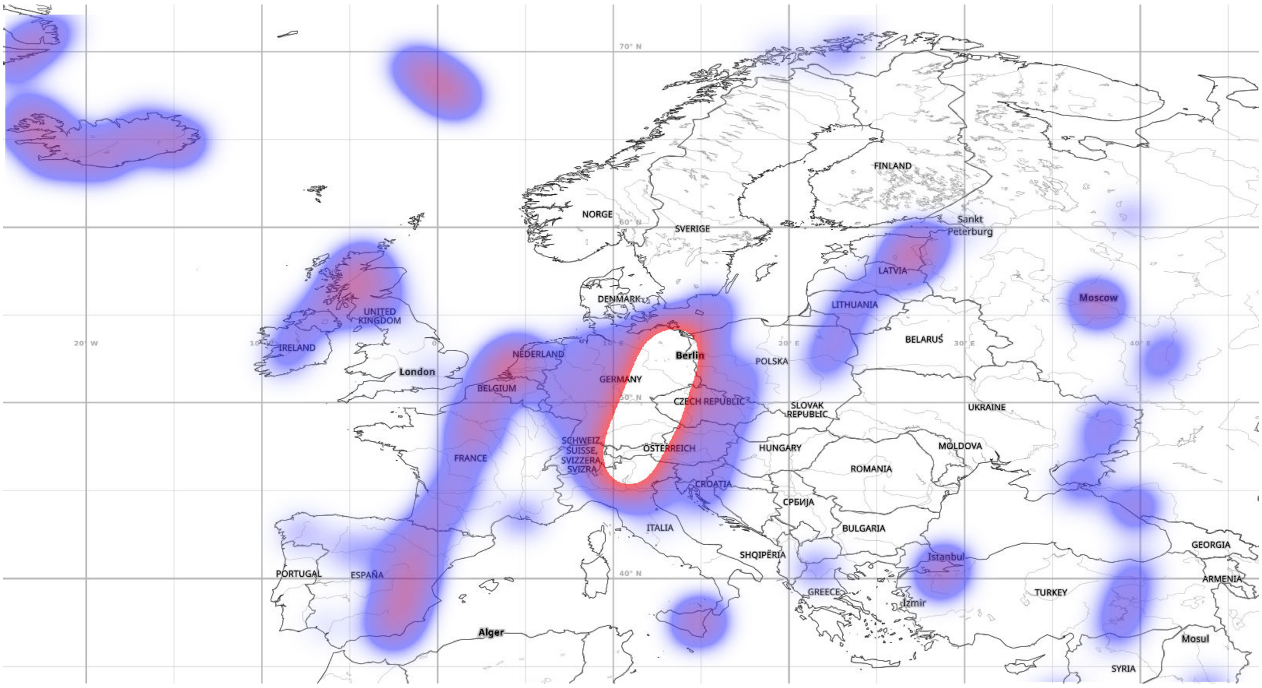

01.10.2022 to 31.12.2022 with 847 tiles

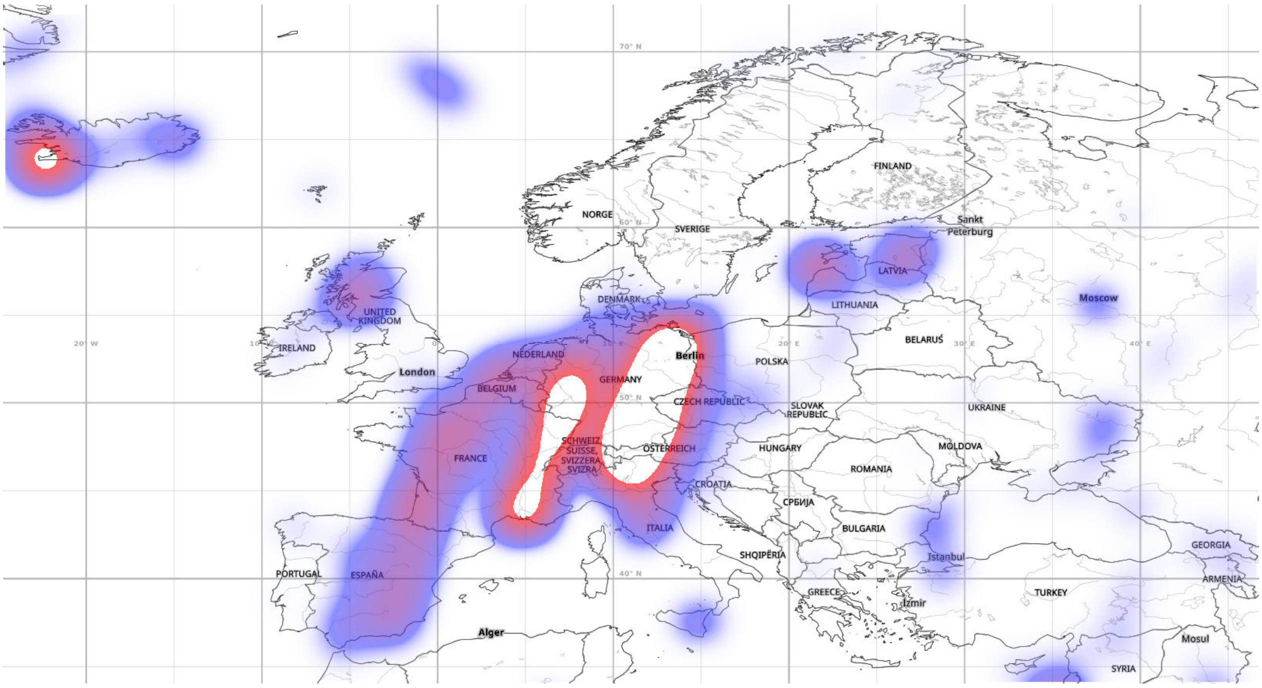

until 31.12.2022 with 2628 tiles

Figure 6-2 Geographic location of all Earth observation tiles archived, Europe

The following figures show the distribution of cloud coverage for the archived products.

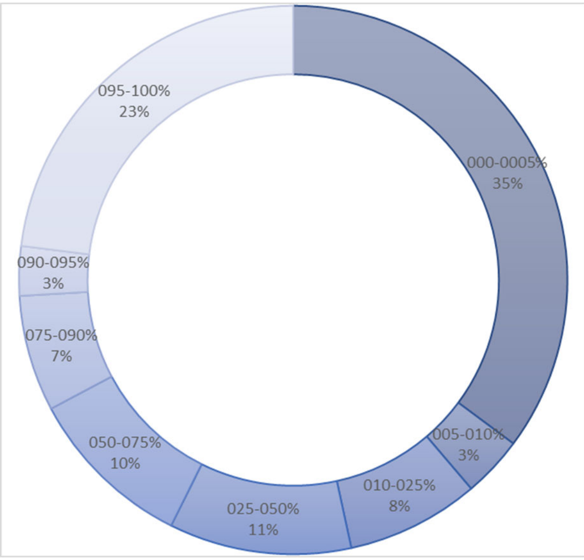

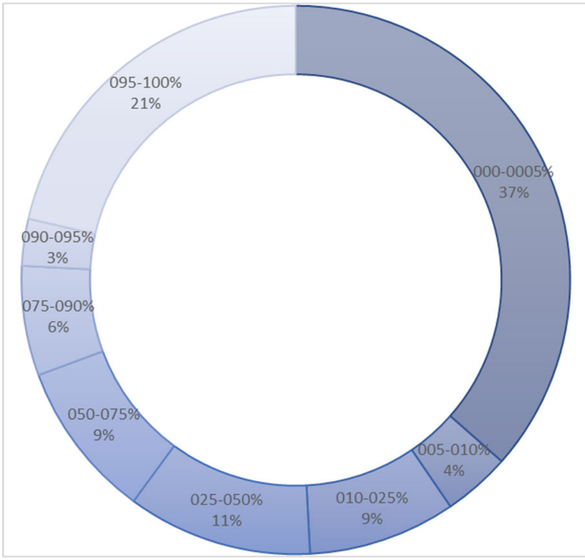

01.10.2022 to 31.12.2022 with 6208 tiles   until 31.12.2022 with 16998 tiles

Figure 6-3 Cloud coverage in [%] of archived Earth observation tiles

The following figures show the distribution of observation angles for the archived products.

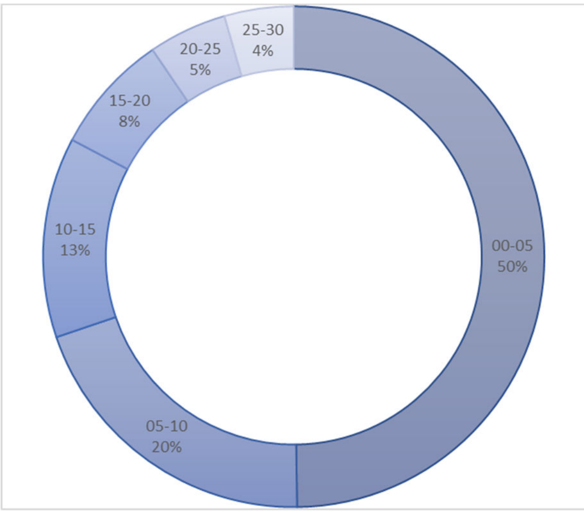

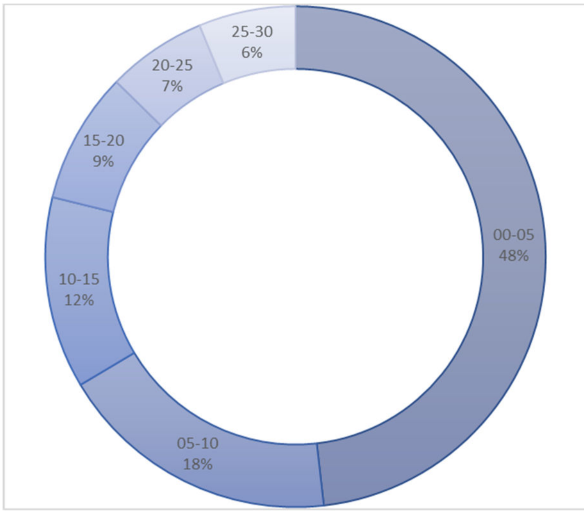

01.10.2022 to 31.12.2022 with 6208 tiles   until 31.12.2022 with 16998 tiles

Figure 6-4 Observation angle of archived Earth observation tiles

6.2 Delivered Observations

The following figures show the distribution of processing level of the delivered products from acquisition orders.

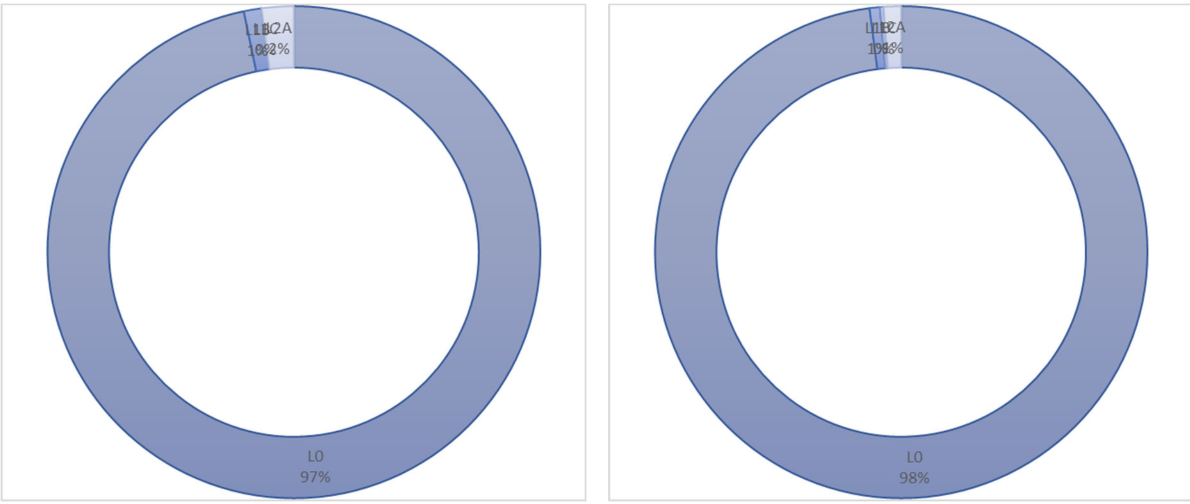

01.10.2022 to 31.12.2022 with 8623 tiles until 31.12.2022 with 17534 tiles

Figure 6-5 Levels of delivered Earth observation tiles from acquisition orders

The following figures show the distribution of processing level and correction type (for L2A) of the delivered products from catalog orders.

01.10.2022 to 31.12.2022 with 2903 tiles until 31.12.2022 with 4810 tiles

Figure 6-6 Levels of delivered Earth observation tiles from catalog orders

7. Detailed Status

7.1 User Interfaces

The user interfaces are related to the Instrument Planning Portal (IPP) and the EOWEB GeoPortal (EGP) for Earth observation planning and accessing via enmap.org. In case of planned outages, they will be communicated at least 24 hours in advance via enmap.org and they will be reported in the Mission Quarterly Report.

The EGP is fully operational, and most parts of the IPP as well. [2] provides an extensive manual to users in particular with respect to the interfaces.

The following limitations in the IPP were applicable during Q4/2022 but are solved as of 31.12.2022:

- The option to submit and view (other users') proposals initially was not yet released [2]. Until 09.12.2022, proposals had to be submitted via e-mail instead via the IPP. Information on the proposal status, i.e. acceptance, had to be communicated to users via e-mail. Since 09.12.2022 the IPP User Interface for Proposal Submission by Users and for Proposal Review is released and operational.
- The option to order Earth observations initially was not yet released [2]. Until 09.12.2022, urgent orders (based on accepted proposals) had to be submitted via e-mail. Products (also) based on these acquisitions were orderable via EGP. Since 09.12.2022 the IPP User Interface for Planning Support and ordering of Earth observations (OR-SPC Point Multi-pass) is released and operational.

The following limitations in the IPP were applicable during Q4/2022 and remain being applicable as of 31.12.2022:

- The option OR-SPC Area Single-pass for ordering of Earth observations by specifying dedicated single acquisitions is not yet released and will be available during Q2/2023. As the alternative option OR-SPC Point Multi-pass is available and fully operational that delay is not blocking for ordering of Earth observations.
- Some obsolete parameters for the specification of Earth observations, e.g. cloud intensity threshold, are still selectable (but without effect). The meaning of the different parameters (obsolete: yes/no) are illustrated in [2]. Those obsolete parameters will be inhibited during Q1/2023.
- Further improvements to the user interfaces based on user feedback are continuously on-going.

7.2 Satellite

Between 13.12.2022 and 13.02.2023 an instrument outage was required as detailed in Section 4.3.

7.2.1 Orbit

The reference orbit is a Sun-synchronous polar orbit with a mean local time of descending node of 11:00 hrs and a repeat cycle of 398 revolutions in 27 days at an altitude of 643 km (lateral deviation of at most 22 km at equator and altitude deviation of at most 6 km).

In the reporting period five orbit maneuvers were performed, all being nominal orbit correction maneuvers. Due to the instrument anomaly the satellite was slightly outside the control rim from mid of December 2022 until mid of January 2023. This limit violation was uncritical though, because no Earth observations and Calibrations were performed. 126 conjunction events were observed, but not collision avoidance maneuver was necessary in the reporting period.

7.2.2 Life-Limited Items

Life-Limited Item	01.10.2022 to 31.12.2022	until 31.12.2022	until end-of-life
Fuel	0.4 kg	2.9 kg	nominal
Battery and Solar Cells	nominal	nominal	nominal
Shutter Usage	2 %	3.1 %	96.9 %
Diffusor Usage	6 %	9 %	91.0 %
Diffusor Exposure	11.4 min	17.4 min	nominal
On-Board Calibration Equipment Usage			
OBCA SPC lamp 1	2.4 %	3.4 %	96.6 %
OBCA RAD lamp 1/LED 1	4.2 %	5.5 %	94.5 %
FPA LEDs 1	1.5 %	2.1 %	97.9 %

Table 7-1 Status of life-limited items

7.2.3 Redundancies

To date, the SWIR wavelength range is covered by SWIR-A (SWIR-B can be activated using a one-time switch mechanism).

All satellite subsystems are using nominal configurations.

7.3 Ground Stations

7.3.1 S-Band

S-Band Ground Stations	01.10.2022 to 31.12.2022		
	Total Passes	Support Passes due to Instrument Anomaly	Failed Passes
Weilheim, Germany Neustrelitz, Germany Inuvik, Canada* O'Higgins, Antarctica* Svalbard, Norway*	408	11*	1

* These passes of these ground stations were ordered in addition to the nominal passes to support the activities (e.g. tests/patches) or on short-notice due to instrument anomaly.

Table 7-2 S-Band Ground Station Passes

7.3.2 X-Band

X-Band Ground Stations	01.10.2022 to 31.12.2022	
	Planned Passes	Performed Passes
Neustrelitz, Germany	275	271

Table 7-3 X-Band Ground Station Passes

It is planned to integrate Inuvik, Canada, as an additional X-Band ground station in Q2/2023. As a result, more data and more flexibility in X-band data reception are expected.

7.4 Processors

[3] provides the product specification and [4], [5], [6], [7] the algorithm theoretical basis for Level 1B, Level 1C and Level 2A (land / water).

In the reporting period (01.10.2022-31.12.2022) there were two processor updates:

1. **Version 01.01.10 (27.10.2022)**
   This version includes the following changes:
   - Corrected variable angles in the rotation matrix (used to transform from coordinate system of HSI to coordinate system of Star Tracker System) to radians. (No effect on quality of products.)
   - Fixed writing of last point of spatialCoverage in metadata.

2. **Version 01.01.11 (22.11.2022)**
   This version includes the following changes:
   - Updated atmospheric correction over water (Level 2A water), to fix an inconsistency with the water products.

The following limitations are applicable as of 31.12.2022:

- The SWIR-A compressor cooler produces a micro-vibration pattern of horizontal stripes on SWIR bands with strong spectral gradients. Still, all spectral and radiometric requirements are within the specification of the mission. An improvement of the processor is planned for mitigating that effect by early 2023.

- The degradations of the VNIR sensor is not uniform across-track. As a result, stronger across-track striping is detected for some observations, in particular at low radiances. An improvement of the processor is planned for mitigating that effect by early 2023.
- The co-registration of the VNIR and SWIR bands is up to 0.4 pixel and exceeds the requirement of the mission of 0.3 pixel. Based on the geometric calibration a co-registration of the VNIR and SWIR bands better than 0.4 pixel is expected in future geometric calibrations.

The following changes are expected to be performed by 31.03.2023:

- Implementation of a de-striping algorithm.
- Implementation of dynamic calibration coefficients to account for rapid change of VNIR calibration as a result of the observed calibration.
- Implement handling of AUX files.
- Change spectral regions for interpolation in Level 2A to 1331.0 nm to 1460.0 nm and 1796.0 nm to 1938.0 nm.
- Improvement in VNIR-SWIR co-registration.

7.5 Calibrations

The continuous degradation of the VNIR sensor was monitored and quantified. The rate of degradation is constantly decreasing as illustrated in Figure 7-1 and it is expected to reach a negligible magnitude in March 2023, pending further monitoring and analysis.

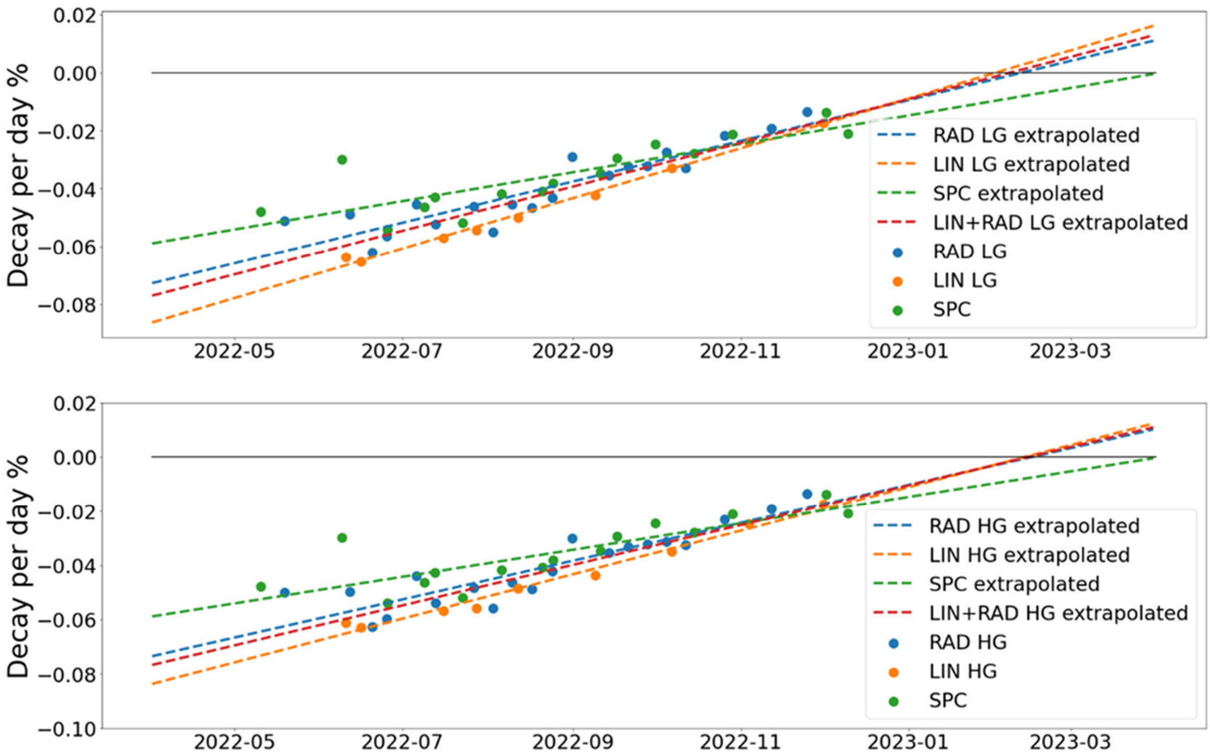

Estimations based on relative radiometric (LMP) and linearity (LIN) (and ALL) calibration measurements for low gain (LG) and high gain (HG). The behavior is linearly extrapolated into 2023.

Figure 7-1 Daily degradation of the VNIR sensor for low gain (top) and high gain (bottom)

The computed radiometric coefficients are illustrated in Figure 7-2 for five selected spectral bands in VNIR. From one Sun calibration to the next, the coefficients are seen to jump, increasing in value over time. It is most pronounced in the edge bands, see e.g. bands 5 and 85.

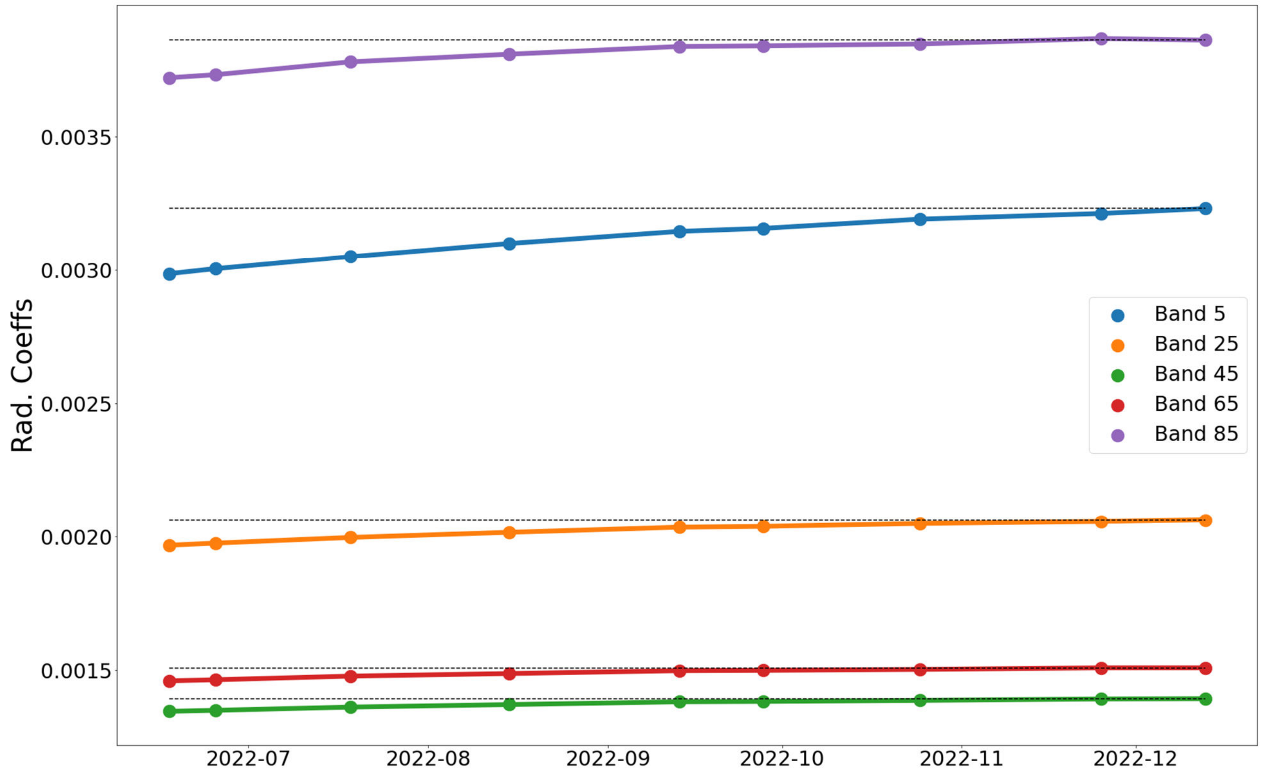

Figure 7-2 **Radiometric coefficients (mW/cm²/sr/µm/Digital Number) for five selected bands**

7.5.1 **Dead Pixels**

Dead Pixels	01.10.2022 to 31.12.2022	
	Number of Pixels	Percent
Total	1921	0.8
VNIR	137	0.2
SWIR	1784	1.2

Table 7-4 **Number and percent of dead pixels**

There are no clusters of more than three spectrally or spatially adjacent dead pixels.

7.5.2 **Spectral Calibration**

Remark: In the following figures, OBCA is abbreviation for On-Board Calibration Assembly for spectral and radiometric calibrations.

Category	01.10.2022 to 31.12.2022	
	Number Archived Observations	Size (in GB)
Total	5	4.5
Spectral Calibration	5	4.5

Table 7-5 **Number and size of archived spectral calibration observations**

The spectral properties – in particular center wavelength (CW) (see Figure 7-3 and Figure 7-4) and full width at half maximum (FWHM) (see Figure 7-5) for each band (spectral coordinate) and pixel (spatial coordinate) – have been characterized, considering all bands and pixels provided in Level 1B, Level 1C and Level 2A products.

The major conclusions of the monitoring of the spectral performance is summarized as follows:

- During the reporting period, five spectral calibration measurements were made. These took place on: 01.10.2022, 15.10.2022, 28.10.2022, 01.12.2022, 09.12.2022.
- The VNIR spectral range in this reporting period was found to be 418.2 nm to 993.0 nm over 91 bands. The average spectral sampling distance was 6.4 nm with a total range of 4.7 nm to 8.2 nm. This meets the requirement for overall wavelength coverage, average spectral sampling distance and spectral sampling distance range.
- The SWIR spectral range in this reporting period was found to be 902.3 nm to 2445.6 nm over 155 bands. The average spectral sampling distance was 10.0 nm with a total range of 7.5 nm to 12.0 nm. This meets the requirement for overall wavelength coverage, average spectral sampling distance and spectral sampling distance range.
- The spectral calibration measurements from this quarter show good temporal stability – all measurements showed a change of less than -0.023% in VNIR and up to 0.009% in SWIR relative to the spectral measurement from 17.09.2022. These changes are below the 0.69 nm requirement between measurements for VNIR and below the 0.86 nm requirement between measurements for SWIR. This meets the requirement for consecutive spectral stability and overall spectral stability.
- FWHM for VNIR and SWIR are shown below but are not recalculated inflight.
- No significant deviations were noticed which would necessitate new calibration or reference tables to be generated in this reporting period.

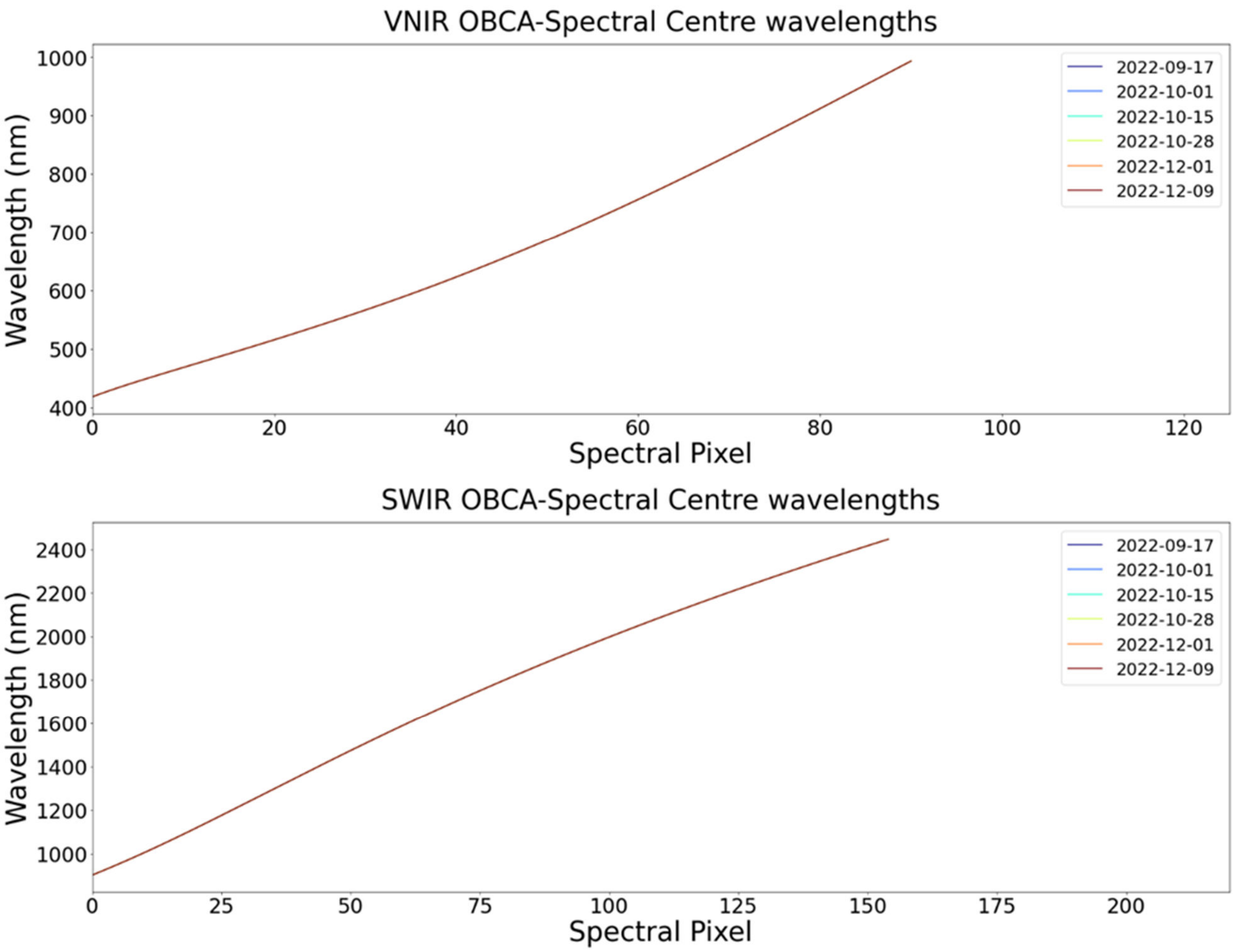

Figure 7-3 VNIR (top) and SWIR (bottom) center wavelength in nm

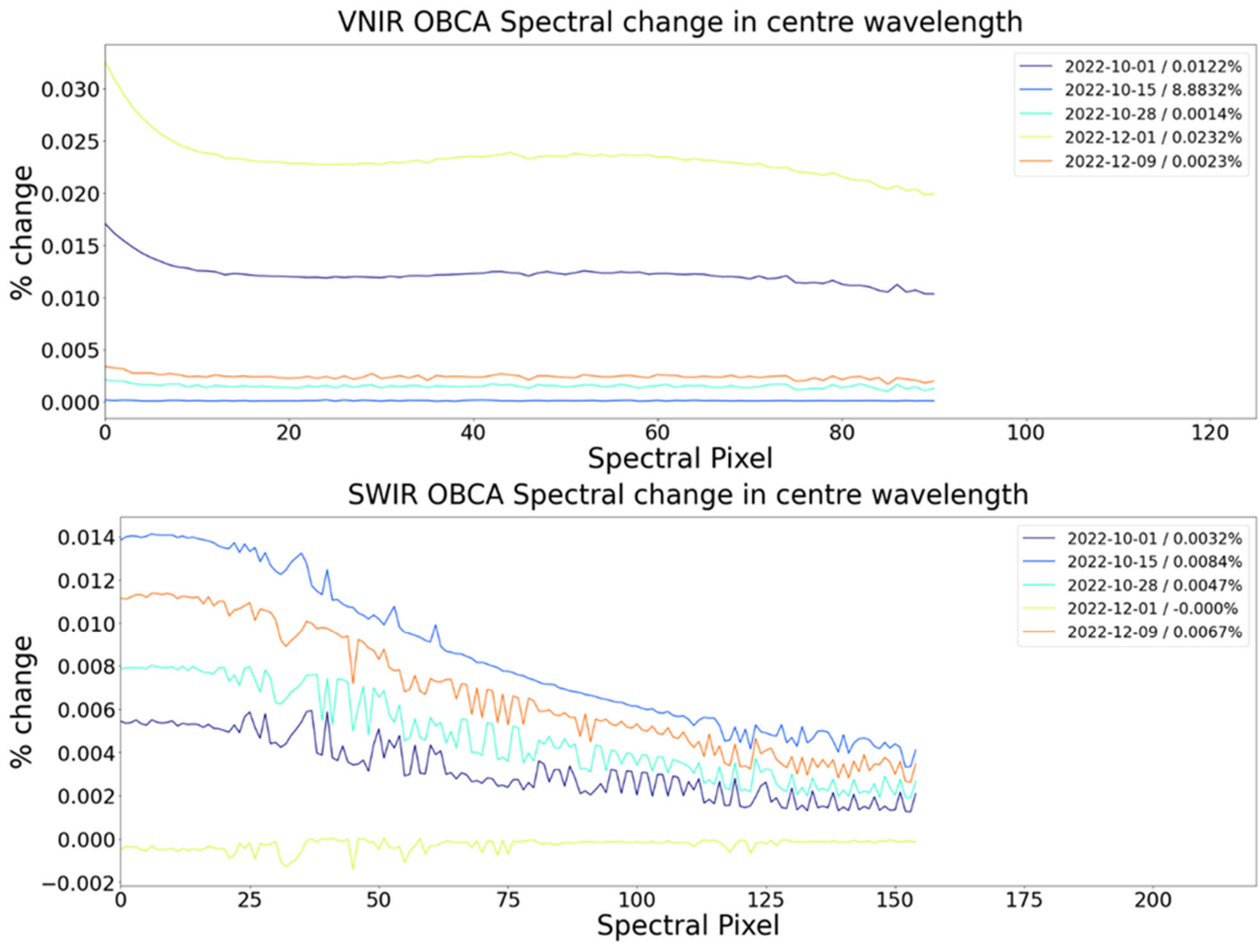

Figure 7-4 Change in center wavelength per spectral pixel for VNIR (top) and SWIR (bottom)

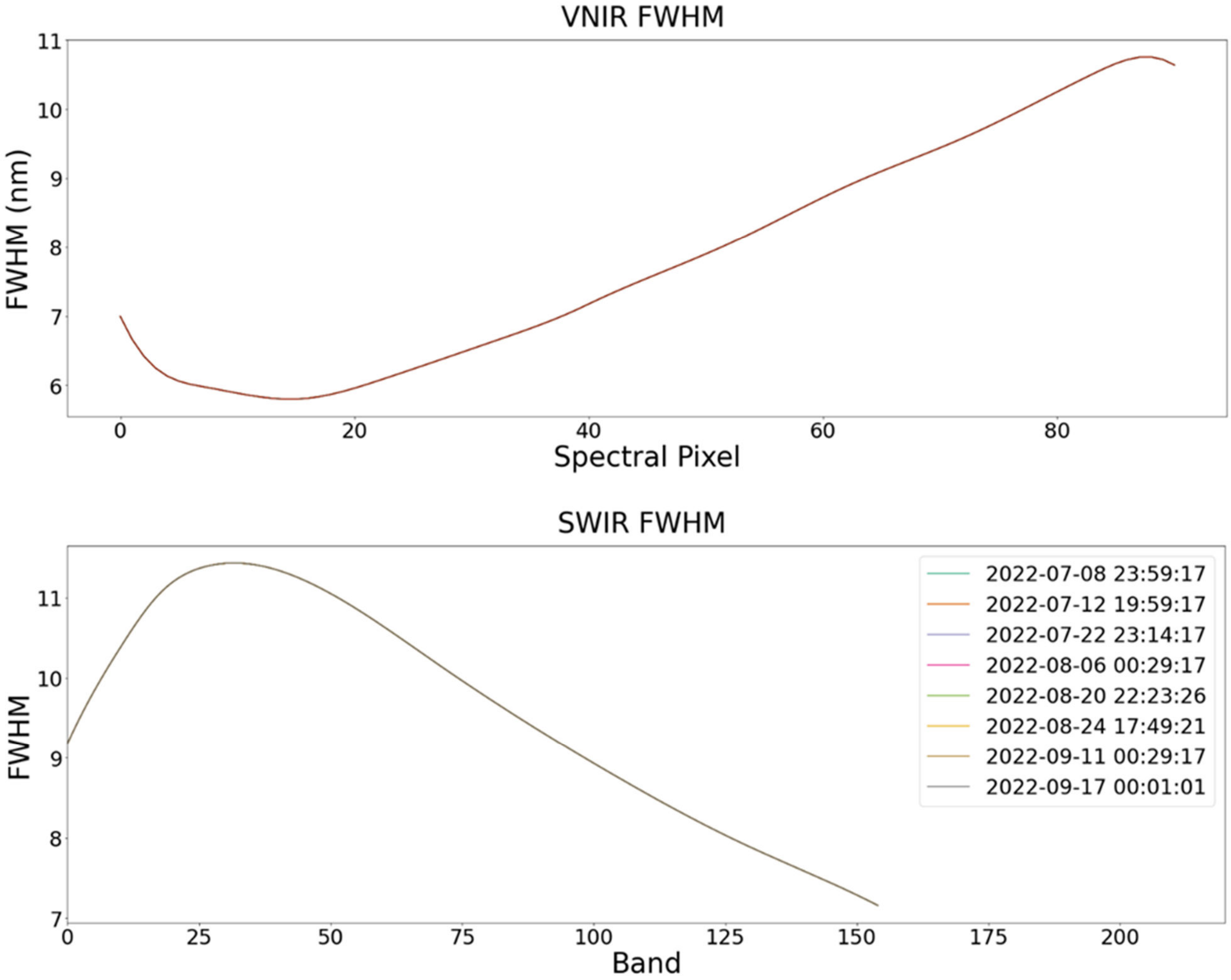

Figure 7-5 VNIR (top) and SWIR (bottom) FWHM in nm

CW and FWHM are available in the spectral calibration tables (see Table 7-6) and System Response Functions (SRF) per band are modelled by a Gaussian shape using those parameters.

Product	Type	Date of Generation	Date of Validity Start	Date of Validity End	Delivered to
Last spectral table from previous quarter	CTB-SPC	ENMAP01-CTB_SPC-20220625T000000Z_V020000_20220701T124609Z	01.07.2022	25.06.2022	-
None for this quarter					

Table 7-6 Generated spectral calibration tables

7.5.3 Radiometric Calibration

Category	01.10.2022 to 31.12.2022	
	Number Archived Observations	Size (in GB)
Total	12	75.7
Deep Space	1	1.3
Rel. Radiometric	5	19.5
Abs. Radiometric	3	3.9
Linearity	3	51

Table 7-7 Number and size of archived radiometric calibration observations

The radiometric properties – characterized in particular by the calibration coefficient for each band (spectral coordinate) and pixel (spatial coordinate) and radiance – during this reporting period are investigated, considering all bands and pixels and radiances provided in Level 1B, Level 1C and Level 2A products.

Both sensors feature two gain settings each. VNIR applies a quantization of 13 bits using a pixel-individual automatic gain switching, where the low gain value is automatically selected, if the signal exceeds a defined threshold. SWIR applies a fixed gain setting, where bands below 1980 nm take the low gain value and bands above 1980 nm take the high gain value.

Radiometric calibration coefficients (see Figure 7-6, Figure 7-7 and Table 7-8) and VNIR RNU (response non-uniformity) (see Figure 7-9) are affected by the degradation of the VNIR sensor and the (expected) change after launch of the SWIR sensor. In-flight, the gain matching coefficients (see Figure 7-8), the SWIR calibration coefficients, and the SWIR RNU (response non-uniformity) (see Figure 7-9) have been stable.

During the reporting period, three Absolute Radiometric calibration measurements were obtained. These took place on: 24.10.2022, 24.11.2022 and 13.12.2022. Owing to the degradation in the VNIR sensor, new calibration and reference tables were created for each new absolute radiometric measurement. The VNIR degradation is partially visible in the reference measurements of the sun. However geometric conditions (sun-earth distance, pointing angle) also play a role in the absolute magnitude so the degradation cannot be quantified with these reference measurements.

As previously stated, the ongoing VNIR degradation affects the absolute Radiometric calibration coefficients. Firstly, the degradation results in an increase in the calibration coefficients themselves to offset the decrease in absolute signal. During this reporting period, the coefficients increased by about 1.1% on average relative to the Sun calibration on 27.09.2022. Regarding RNU, the degradation features are visible in the focal plane. Looking at the average along across track pixels, the RNU correction has decreased on the sides and increased in the center, where the highest degradation takes place. Lastly, the Gain Matching correction has been relatively stable during this reporting period. The SWIR sensor has shown good stability during this reporting period, with no significant changes in the gain matching, RNU or radiometric calibration coefficients.

Regarding the total change in calibration corrections as a result of the VNIR degradation, almost all pixels experienced a change of less than 2.5% between consecutive measurements as set in requirement [HSI-POSR-0410]. Only one pixel exceeded this value and this pixel was already marked as dead during preflight assessment. No SWIR pixels experienced a change of more than 2.5% between consecutive absolute calibration measurements. Due to the degradation in the VNIR sensor, new calibration and reference tables were created for each new absolute radiometric measurement. The size of the degradation has been decreasing during this reporting period and it is smaller than it was in the last reporting period

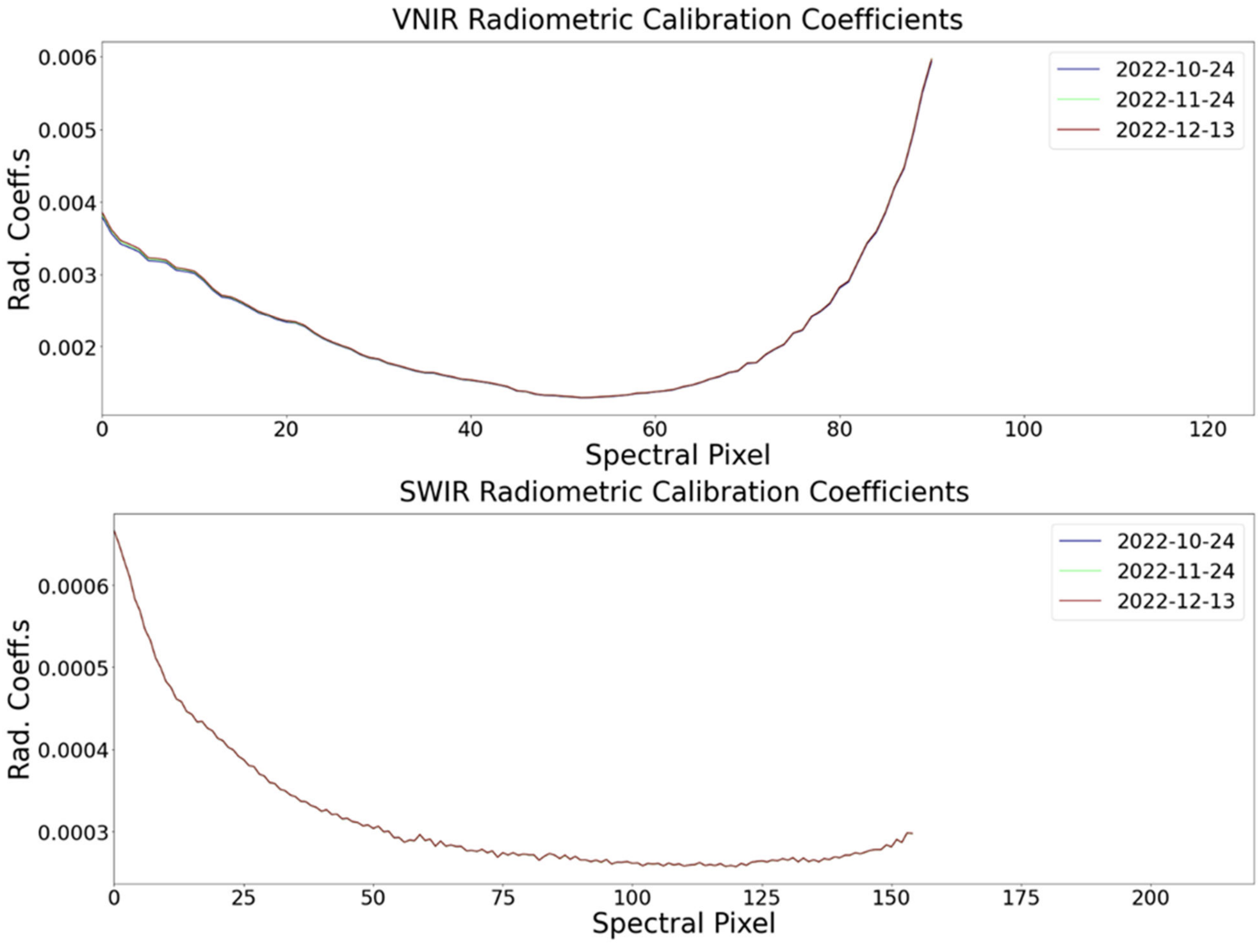

Figure 7-6 VNIR (top) and SWIR (bottom) calibration coefficient in mW/cm²/sr/µm

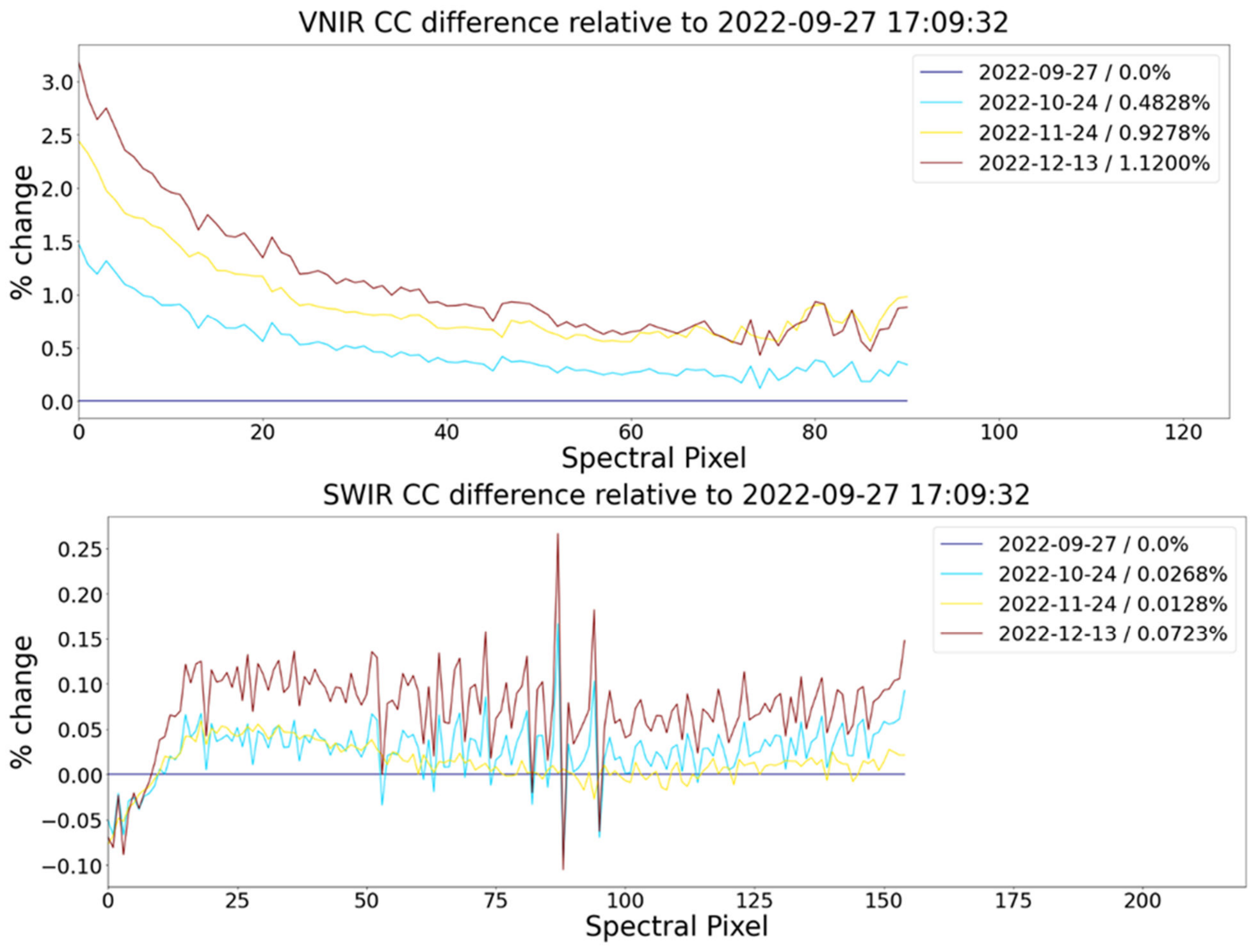

averaged in spectral pixels for all observations in the reporting period 01.10.2022 to 31.12.2022 relative to the observation on 27.09.2022

Figure 7-7 Percentage change in VNIR Calibration Coefficients (top) and SWIR Calibration Coefficients (bottom)

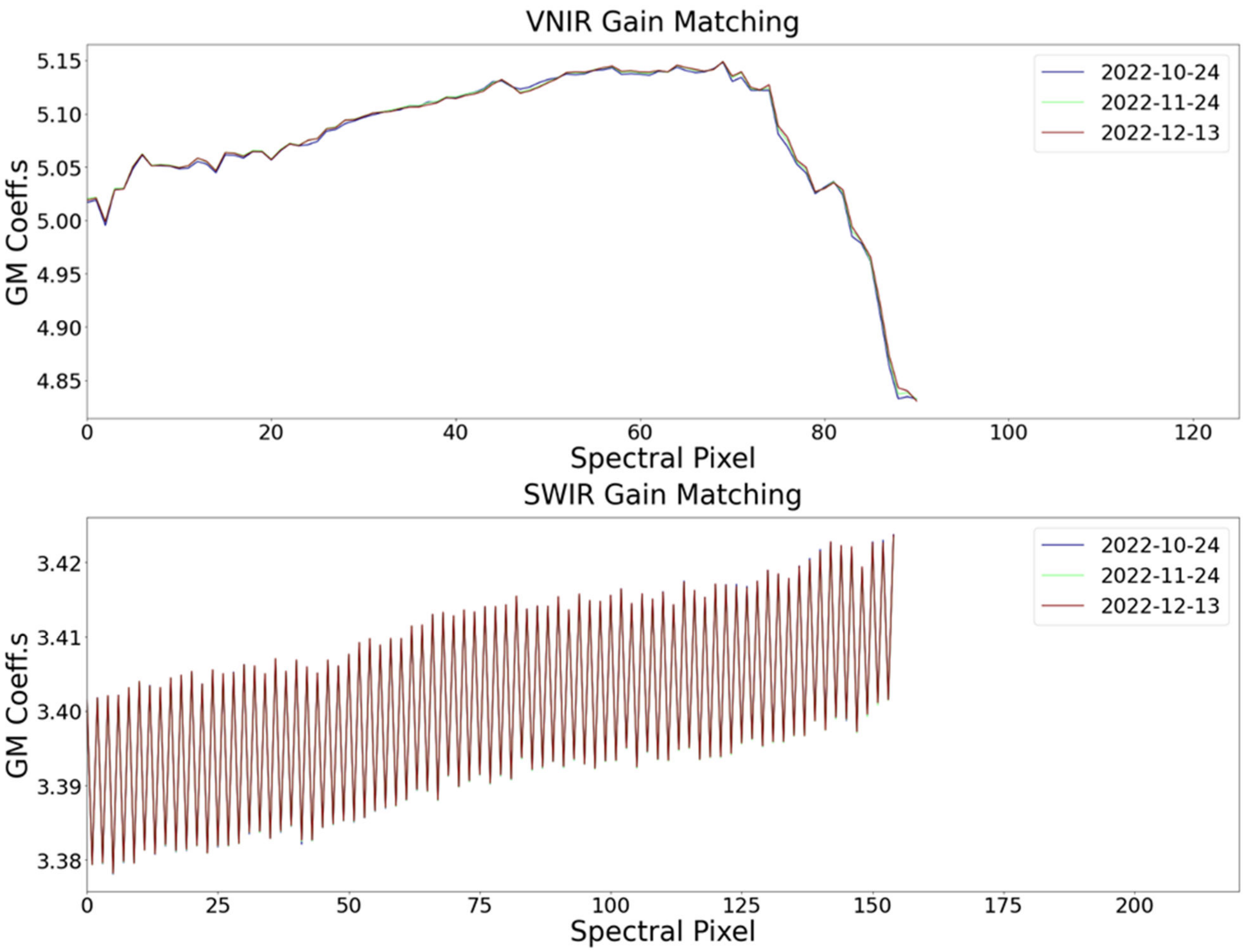

Figure 7-8 VNIR (top) and SWIR (bottom) gain matching calibration coefficients

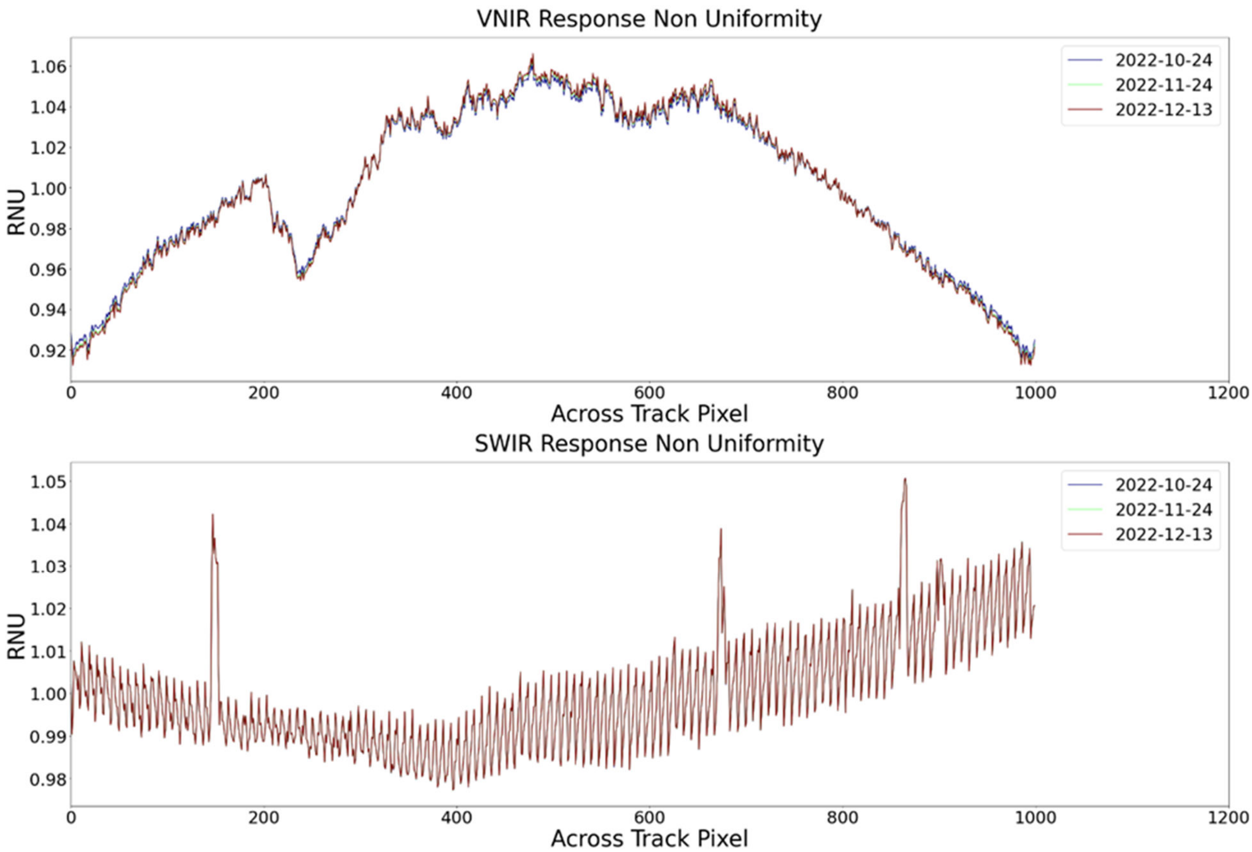

Figure 7-9 VNIR (top) and SWIR (bottom) response non-uniformity coefficients

The Signal-to-Noise Ratio (SNR) is derived from the Linearity reference measurements. This is not a perfect set-up for the assessment of the SNR as the linearity measurements only cover a single wavelength and light level at increasing integration times. However, it is well constrained, covering a wide range of radiances including the levels of the solar reference spectrum (30% reflectance, 30° sun incidence angle, 21 km visibility, target 500 m above sea level). The lamp reference measurements are not used, as the reference spectrum is not well covered at the radiances of the lamp and extrapolation would be required to test the performance at the SNR requirements: SNR greater than 500 at 495 nm in VNIR for the solar reference spectrum value; and SNR greater than 150 at 2200 nm in SWIR for the reference spectrum.

For the VNIR sensor, the Signal-to-Noise Ratio has changed during commissioning phase as a result of the ongoing degradation. Nevertheless, the high gain and low gain measurements imply that the SNR in each gain are above the requirement of the reference spectrum at 495 nm. In the case of VNIR low gain, the SNR was found to be 630 for the measurement on 30.11.2022. This value is the practically the same as the one reported in previous quarterly report and indicates how this VNIR degradation is reducing over time.

For the SWIR sensor, both gains are above the requirement at 2200 nm, giving an SNR value of 350 in high gain mode from 30.11.2022. Figure 7-10, Figure 7-11, Figure 7-12 and Figure 7-13 show SNR contour maps for each sensor and gain, based on observed linearity measurements from 30.11.2022, and the solar reference spectrum is plotted to show how the SNR is derived in each case.

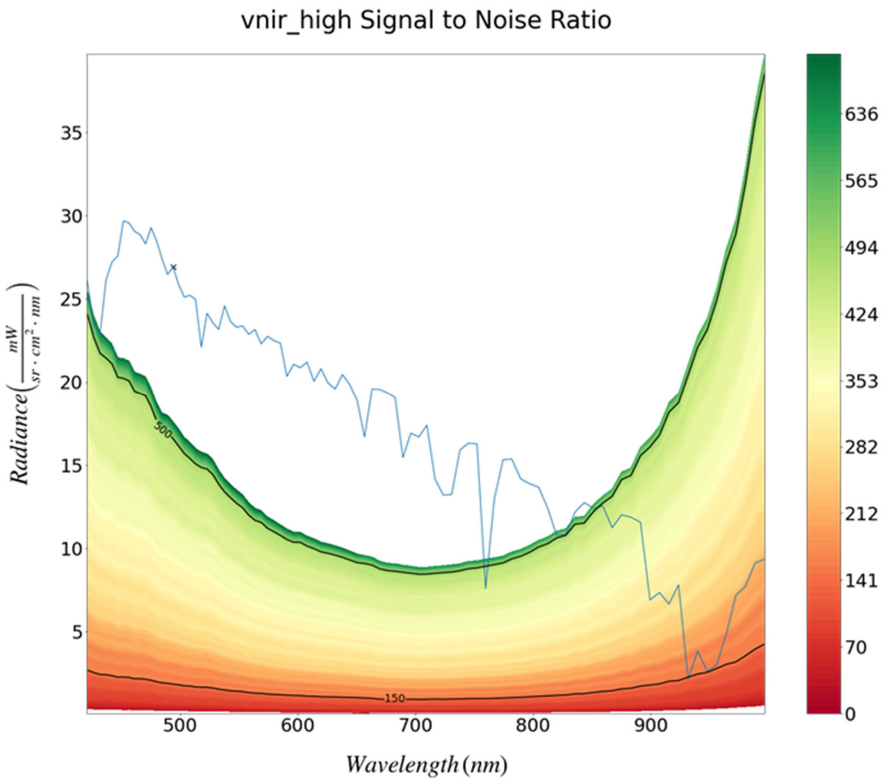

blue line: solar reference spectrum (30% reflectance, 30° sun incidence angle, 21 km visibility, target 500 m above sea level). black cross: position of the requirement on the reference spectrum. black line: contour lines with SNR values of 150 and 500

Figure 7-10 SNR contour map for VNIR high gain from the LED linearity observations, 30.11.2022

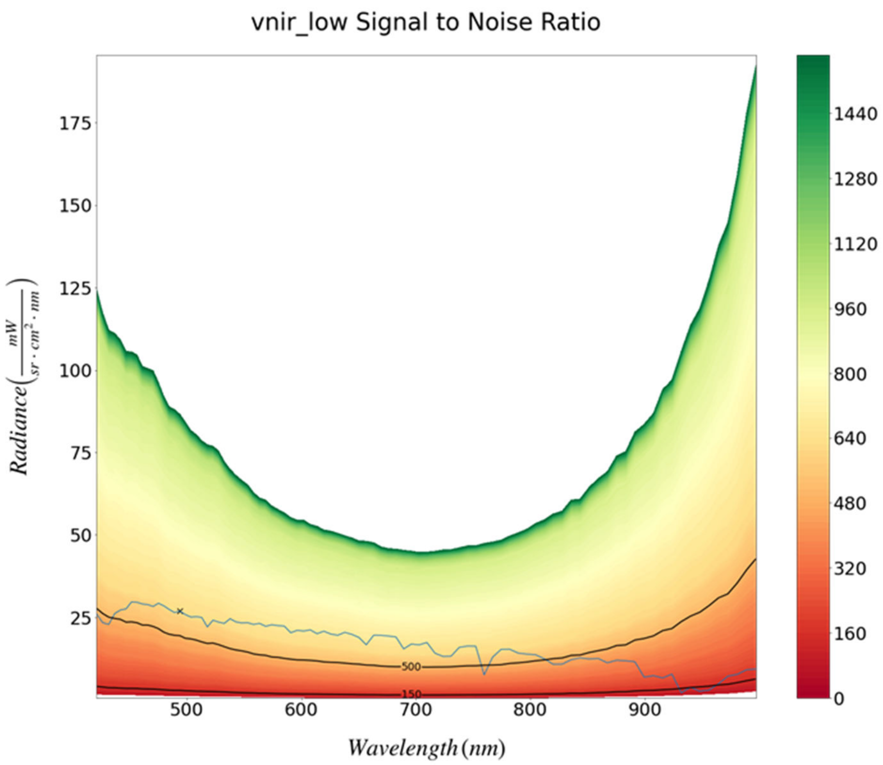

blue line: solar reference spectrum (30% reflectance, 30° sun incidence angle, 21 km visibility, target 500 m above sea level). black cross: position of the requirement on the reference spectrum. black line: contour lines with SNR values of 150 and 500

Figure 7-11 SNR contour map for VNIR low gain from the LED linearity observations, 30.11.2022

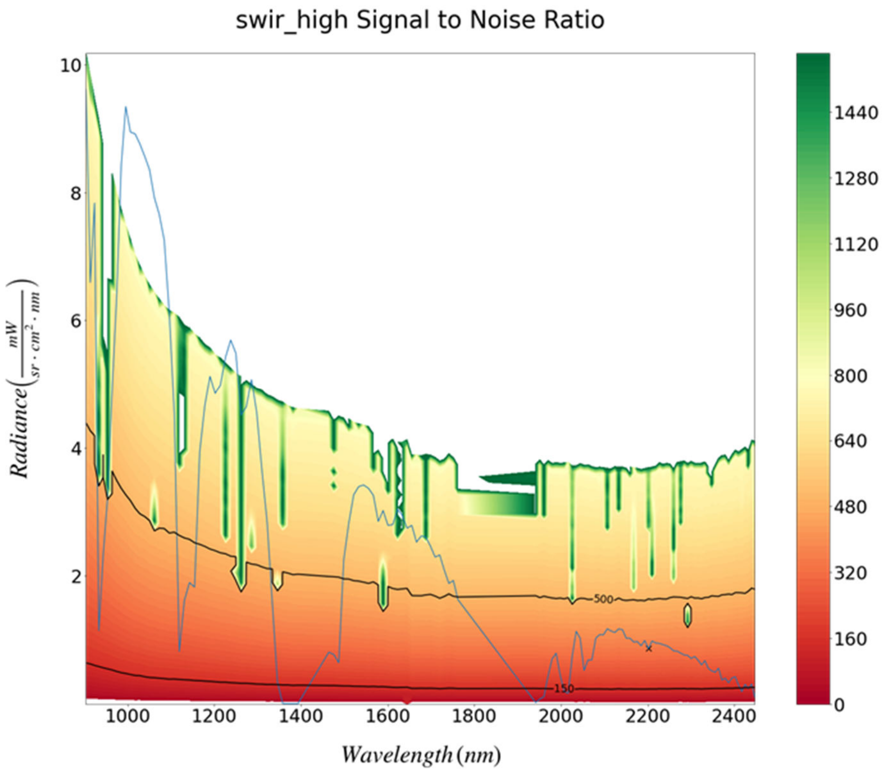

blue line: solar reference spectrum (30% reflectance, 30° sun incidence angle, 21 km visibility, target 500 m above sea level). black cross: position of the requirement on the reference spectrum. black line: contour lines with SNR values of 150 and 500

Figure 7-12 SNR contour map for SWIR high gain from the LED linearity observations, 30.11.2022

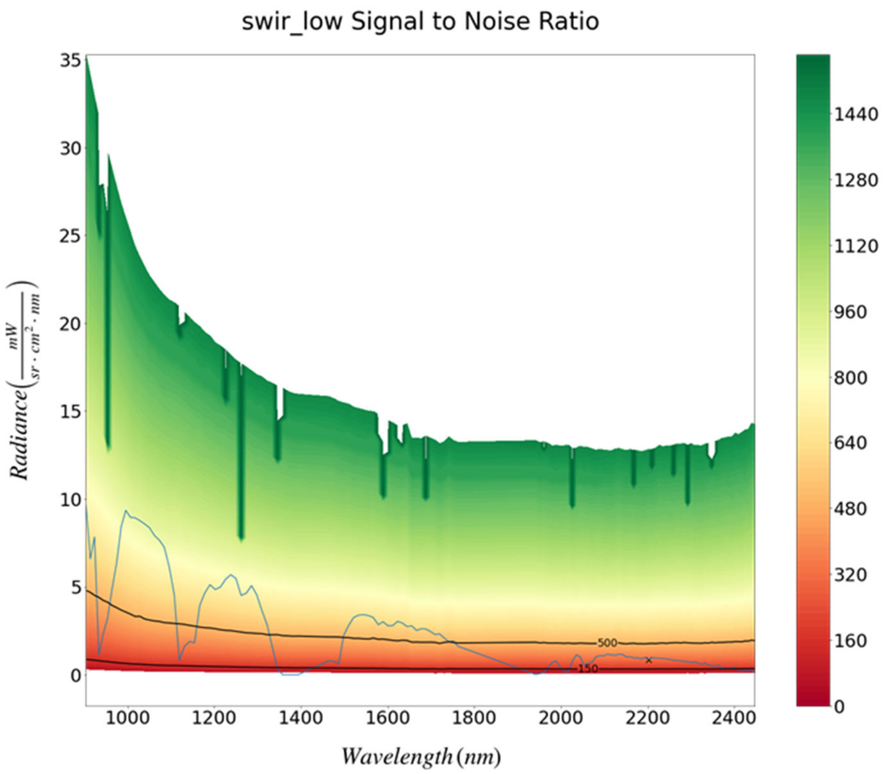

blue line: solar reference spectrum (30% reflectance, 30° sun incidence angle, 21 km visibility, target 500 m above sea level). black cross: position of the requirement on the reference spectrum. black line: contour lines with SNR values of 150 and 500

Figure 7-13 SNR contour map for SWIR low gain from the LED linearity observations, 30.11.2022

Product	Type	Date of Generation	Date of Validity Start	Date of Validity End	Delivered to
ENMAP01-CTB_RAD-20220928T000000Z_V020000_20220928T165957Z	CTB_RAD	28.09.2022	28.09.2022	25.10.2022	DIMS (from last report)
ENMAP01-CTB_RAD-20221025T000000Z_V020000_20221025T062338Z	CTB_RAD	25.10.2022	25.10.2022	25.11.2022	DIMS
ENMAP01-CTB_RAD-20221125T000000Z_V020000_20221128T080837Z	CTB_RAD	28.11.2022	25.11.2022	14.12.2022	DIMS
ENMAP01-CTB_RAD-20221214T000000Z_V030000_20221215T085151Z	CTB_RAD	15.12.2022	14.12.2022	-	DIMS
ENMAP01-REF_SUN-20220928T000000Z_V020000_20220928T165957Z	REF_SUN	28.09.2022	28.09.2022	25.10.2022	DIMS (from last report)
ENMAP01-REF_SUN-20221025T000000Z_V020000_20221025T062338Z	REF_SUN	25.10.2022	25.10.2022	25.11.2022	DIMS
ENMAP01-REF_SUN-20221125T000000Z_V020000_20221128T080837Z	REF_SUN	28.11.2022	25.11.2022	14.12.2022	DIMS
ENMAP01-REF_SUN-20221214T000000Z_V030000_20221215T085151Z	REF_SUN	15.12.2022	14.12.2022	-	DIMS

Table 7-8 Generated radiometric calibration tables

7.5.4 Geometric Calibration

A calibration table was created on 18.10.2022 with a validity start date on 03.11.2022. A total of 175 Level 1B products were selected for the calibration. As the blunder detection thresholds were very strict in the matching process, not for all of them a sufficient number of GCP was found to be included in the calibration. In consequence, for the VNIR calibration 148 tiles could be used while for the SWIR calibration 128 tiles could be used.

Type of Calibration Table	ID of Calibration Table	Date of Generation	Date of Validity Start	Date of Validity End
CTB-GEO	ENMAP01-CTB_GEO-20221103T000000Z_V010100_20221018T091032Z	2022-10-18T09:10:32.490900Z	2022-11-03T00:00:00.000000Z	-

Table 7-9 Generated geometric calibration tables

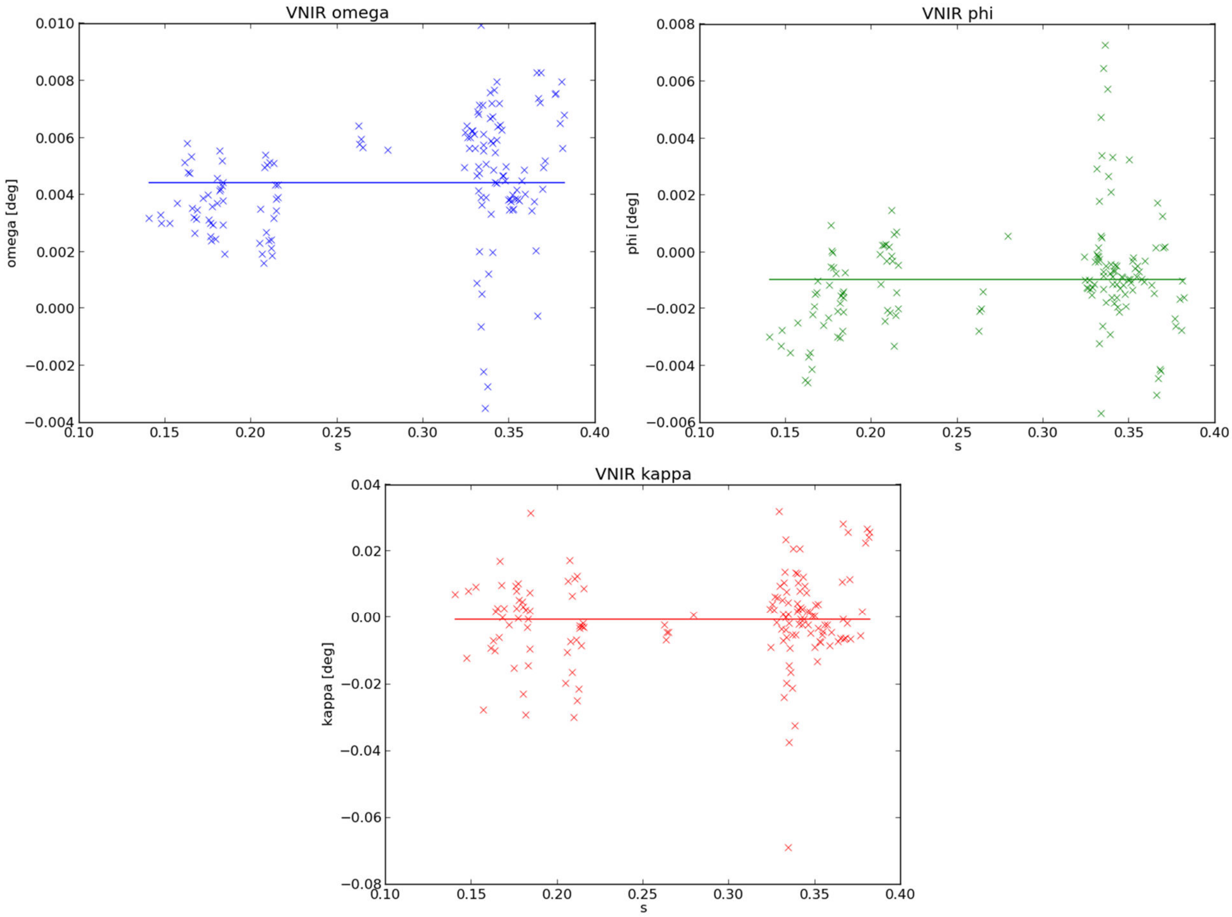

The residuals for these fits are 0.00063652 deg (Omega), 0.00057146 deg (Phi) and 0.0272919 deg (Kappa).

Figure 7-14 VNIR boresight angles Omega (top left, blue), Phi (top right, green) and Kappa (bottom, red) and polynomial fit

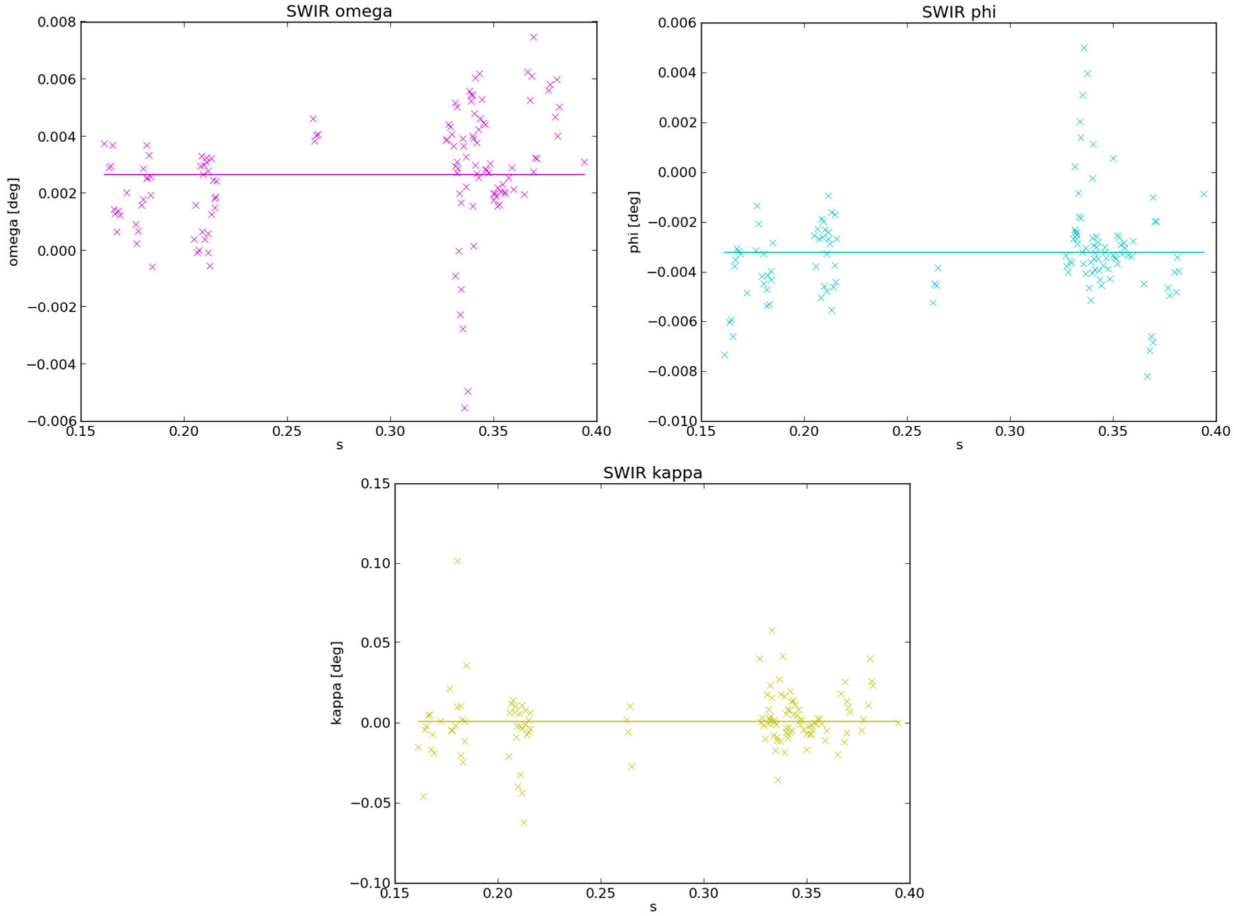

The residuals for these fits are 0.00048465 deg (Omega), 0.00044005 deg (Phi) and 0.04392915 deg (Kappa).

Figure 7-15 SWIR boresight angles Omega (top left, purple), Phi (top right, cyan) and Kappa (bottom, yellow) and polynomial fit

7.6 Internal Quality Control

7.6.1 Archive

Within the timeframe between 01.10.2022 and 31.12.2022, 970 datatakes with a total of 6158 tiles were acquired and archived (remark: additional datatakes acquired during this period but for which the archiving is pending might be missing in the statistics).

The overall quality rating statistics are listed in Table 7-10, and are detailed for the VNIR and SWIR detector in Table 7-11, showing a nominal performance rating for the given quality thresholds.

In addition, the rating for the atmospheric conditions for the scenes are depicted in Table 7-12. When setting the atmospheric quality rating in relation to the illumination conditions (i.e., Solar Zenith Angle (SZA)) during data acquisition, over 40% of the “reduced quality” ratings and over 44% of the “low quality” ratings can be related to low Sun angles.

Parameter	Value	Percentage	Absolute
overallQuality	Nominal	91%	5594
	Reduced	1%	51
	Low	8%	513

Table 7-10 Reduced and low quality rating statistics (overall)

Parameter	Absolute	Sub-Parameter	Absolute
overallQuality = Reduced	51		
		Thereof with qualityVNIR nominal	34
		Thereof with qualitySWIR nominal	1
overallQuality = Low	513		
		Thereof with qualityVNIR nominal or reduced	0
		Thereof with qualitySWIR nominal or reduced	513

Table 7-11 Reduced and low quality rating statistics (VNIR & SWIR)

Parameter	Value	Percentage
QualityAtmosphere	Nominal	29%
	Reduced	25%
	Low	45%

Table 7-12 Reduced and low quality rating statistics (atmosphere)

The following limitations are applicable as of 31.12.2022:

- Inconsistent sensitivity and thresholding of striping flagging in data quality control for archived products.
- Inconsistent anomaly flagging of SWIR for band-to-band fluctuations and micro-vibrations.
- Inconsistent sensitivity and thresholding of saturation flagging in data quality control for archived products.

The planned re-processing of the archive considers these inconsistencies.

7.6.2 Level 1B

7.6.2.1 Radiometric Performance

Indications for defective / de-calibrated detector elements

Using the Detector Map components, an offline check of possibly defective or de-calibrated detector elements is conducted. In particular, if a detector element is identified as “possibly defective” in at least 75%

of the useful tiles. Within the given reporting period, the following indications for defective pixels are found for the VNIR and the SWIR camera:

VNIR (total of 5181 tiles, with 4684 suitable for analysis):

Band	Cross-track element
85	14
89	395

SWIR (total of 5181 tiles, with 4648 suitable for analysis):

Band	Cross-track element	Band	Cross-track element
2	235, 286, 593, 673	49	311, 344, 395
4	362, 363, 418	50	154, 155
5	687	52	97
7	910	53	602, 941
8	801	55	221, 965
9	124	57	632, 922
11	715	58	89, 90
14	29, 684	60	312
16	535	62	123
19	84	71	801, 844, 845
20	84	91	973
28	104	92	677, 973
29	855, 928	96	341, 819
30	7, 360, 855	101	318
31	360	106	107
33	560	107	265, 764
38	241, 919	108	886
39	486	111	315
47	511	118	837
48	218		

Indications for increasing dead detector elements

Within the given reporting period, the statistics for dead pixels are provided in Table 7-13 and Table 7-14. When comparing these numbers to the estimates in the EN-GS-RPT-1702 Radiometric Calibration Report, one must bear in mind that the latter is based on the full detector readout configuration, while the numbers provided in the following are related to the standard readout configuration as provided in the user product. Because of the smaller readout area, these following dead pixel numbers are lower in comparison.

Parameter	Value (number of pix)	Percentage of tiles
DeadPixelsVNIR	2 (*)	12% (*)
	137	88%

Table 7-13 Dead pixel statistics, VNIR

(*): note that the DeadPixelMap was not updated for these datasets, and value will change after re-processing of archived data

Parameter	Value (number of pix)	Percentage of tiles
DeadPixelsSWIR	680 (*)	12% (*)
	1531	88%

Table 7-14 Dead pixel statistics, SWIR

(*): note that the DeadPixelMap was not updated for these datasets, and value will change after re-processing of archived data

Saturation and radiance levels outside nominal range
Within the given reporting period, no indications for increased saturation defects are found for the VNIR and the SWIR camera (see Table 7-15 and Table 7-16).

Parameter	Value (per mille of scene)	Percentage of tiles
SaturationCrosstalkVNIR	0	93%
	> 0 per mille	7%
	> 10 per mille	1%

Table 7-15 Saturation statistics, VNIR

Parameter	Value (per mille of scene)	Percentage of tiles
SaturationCrosstalkSWIR	0	96%
	> 0 per mille	4%
	> 10 per mille	0%

Table 7-16 Saturation statistics, SWIR

7.6.2.2 Spectral Performance

For the analysis of the spectral stability, the Detector Maps of all Earth datatakes acquired in the reporting period were used. Note that no smile correction was applied, so the analysis shows only on the instrument characteristics. At the wavelengths of stable atmospheric features (760 nm Oxygen absorption and 2060 nm CO2 absorption), simulations of spectral shifts were carried out by resampling the absorption in the interval of +/- 3.0 nm with steps of 0.05 nm. Then the signal of the Detector Maps and the simulated shifted absorptions were normalized, and a least-square fit was used where the sensed absorption matches the simulations. Also, an additional polynomial fitting was applied, as especially the CO2 absorption band region has low signal an is thus significantly influenced by noise.

When repeating this analysis for many Detector Maps, then the spectral behavior over time can be addressed (Figure 7-16, Figure 7-18). More important is the standard deviation of the shift, as this represents the spectral stability within the given period [AR-5]. As shown in Figure 7-17 and Figure 7-19, the standard deviation (1σ) at 760 nm is better than 0.25 nm for all cross-track elements, and better than 0.65 nm at 2060 nm. Also the cross-track shape shows little variation; in case of the VNIR, the stability is equally good for all cross-track elements, while for the SWIR the shape is similar to the detected center wavelengths deviation.

In summary, these findings agree well with the instrument performance estimated during the Commissioning Phase [IR-01], with the estimated mean shifts and the standard deviation of the SWIR being slightly higher.

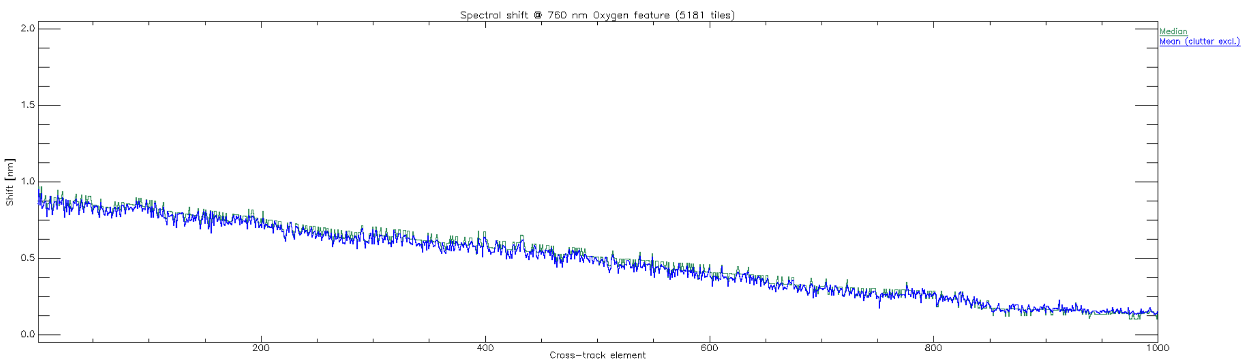

Figure 7-16 VNIR estimated spectral shift of the bands at 760 nm w.r.t. the nominal band center (same baseline as in CP)

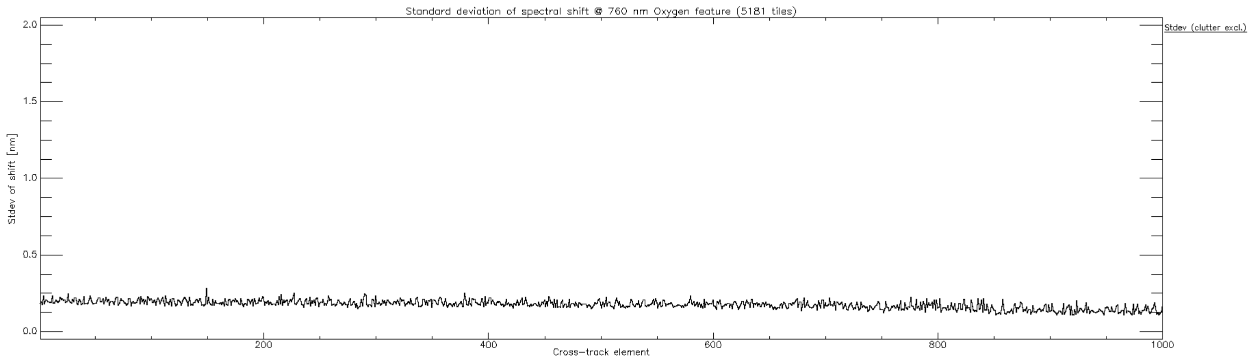

Figure 7-17 VNIR relative spectral stability at 760 nm, expressed at 1 sigma; 5181 tiles

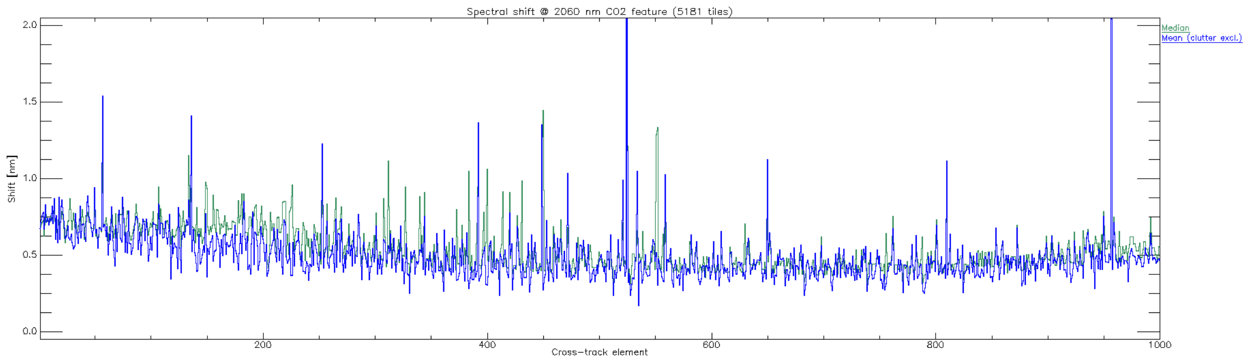

Figure 7-18 SWIR estimated spectral shift of the bands at 760 nm w.r.t. the nominal band center (same baseline as in CP)

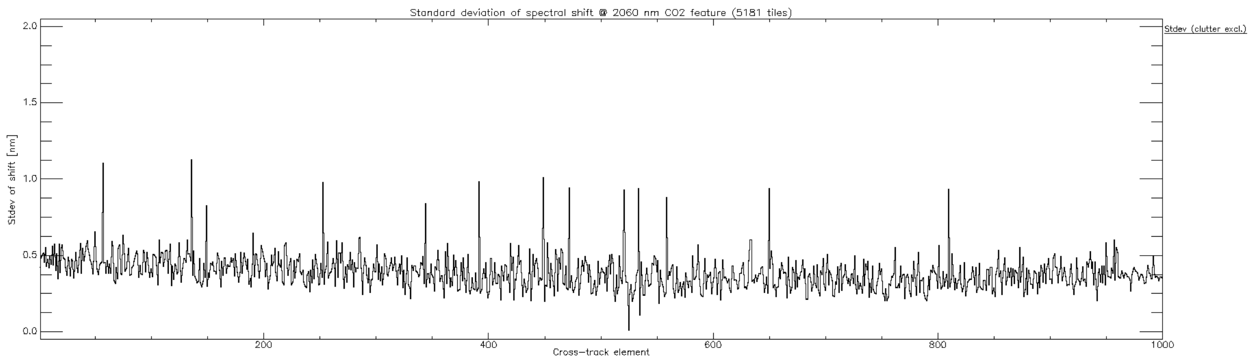

Figure 7-19 SWIR relative spectral stability at 2060 nm, expressed at 1 sigma; 5181 tiles

7.6.2.3 Image artifacts

Apart from the three known radiometric artefacts, no indications for an increase in general radiometric/spectral problems are found for the VNIR and the SWIR cameras. The known artefacts are indicated below.

1. **Image Artefacts: Striping and Fixed Pattern Noise**

For a detailed analysis of the cross-track striping a total of 2770 calibrated detector maps (derived before dead pixel interpolation) were compiled. As shown in Figure 7-20 for VNIR, the spectral and especially the across-track profiles are not smooth even when averaged over approx. 2.8 million frames, but show a spiking pattern. Within the images, these spiking patterns appear as striping artefacts, i.e. a fixed pattern noise affecting all frames of one image column.

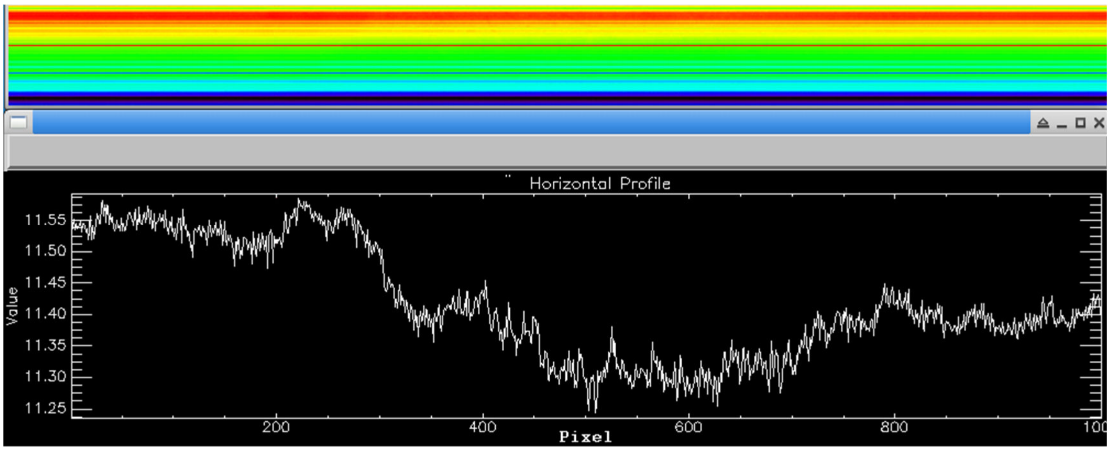

Figure 7-20 VNIR, mean of all Detector Maps, with typical across-track profile in mW/cm²/sr/µm

The magnitude of this fixed-pattern noise is the mean absolute difference of the noise over all 2770 observations.

The relative magnitude is 0.2% for band at wavelengths shorter than 870 nm and increases for bands at wavelengths affected by fringing, that is detailed later, and under the influence of atmospheric water vapor absorption. Also, the peak at the band at wavelength 750 nm is due to small spectral shifts of the oxygen absorption in this wavelength range. Furthermore, the slight increase towards the bands at shortest wavelengths indicates the likely presence of some random noise.

In order to analyze the impact of the radiance level, the original detector maps were split by the median overall observation radiance. The analysis was then repeated for both groups with 1385 detector maps each. As the arithmetic mean is calculated for each band individually, the overall radiance level should not matter, just the change in percentage.

Figure 7-21 illustrates that lower radiance observations show a higher pixel-by-pixel difference than higher radiance observations. As this is the average over approx. 1.4 million frames each, the effects of random noise should be significantly reduced and not dominate the analysis. The exceptions are the bands at wavelengths longer than 870 nm of VNIR, where fringing adds a random component, and bands significantly affected by atmospheric absorptions also add randomness.

The analysis was carried out for both VNIR and SWIR, as shown in Figure 7-21 and Figure 7-22. The magnitude for the VNIR is approx. 0.2% for the higher radiance group, and approx. 0.4% for the lower radiance group disregarding the bands affected by fringing and/or atmospheric absorption. For SWIR, the bands at wavelengths smaller than 1350 nm show similar low across-track pixel variations, which increase for higher radiance observations up to approx. 1.0% in the highest bands, which are increasingly influenced by random noise. For low radiance observations, variations for SWIR are higher by a factor of approx. 2.

For both VNIR and SWIR, the lower radiance grouping shows a higher pixel-to-pixel difference (i.e. striping indication) than the higher radiance group. This is partially due to the remaining random noise which is relatively larger at lower radiance levels. This is an indication that the magnitude of striping is somehow linked to the overall radiance level, possibly pointing to an additive striping effect: Adding a fixed (radiance) part to high radiances results in small pixel-to-pixel variation in [%], while adding the same amount of striping to low radiances results in higher variations in [%]).

Note that for SWIR, there is a clear transition between low and high gain at band at wavelength 1980 nm, indicating an influence of the SWIR gain on the results. Especially for low radiance observations, the high gain range of the SWIR shows a larger indication for striping / fixed pattern noise, even considering the increased influence of random noise in the analysis.

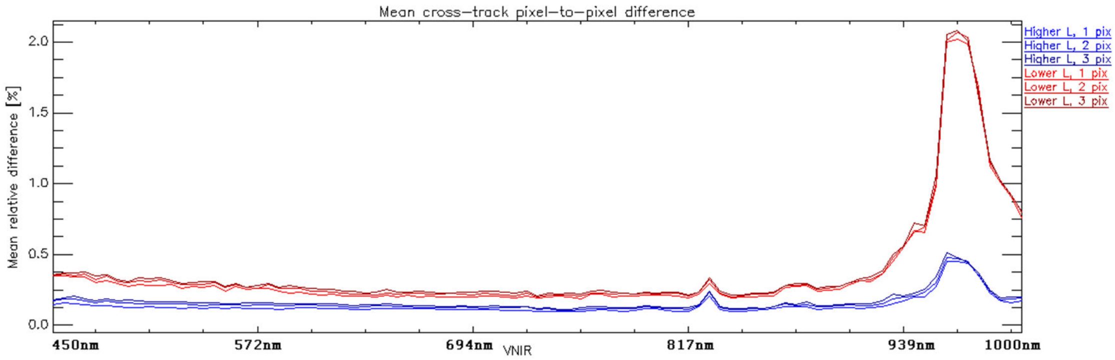

Figure 7-21 VNIR mean cross-track pixel-to-pixel difference

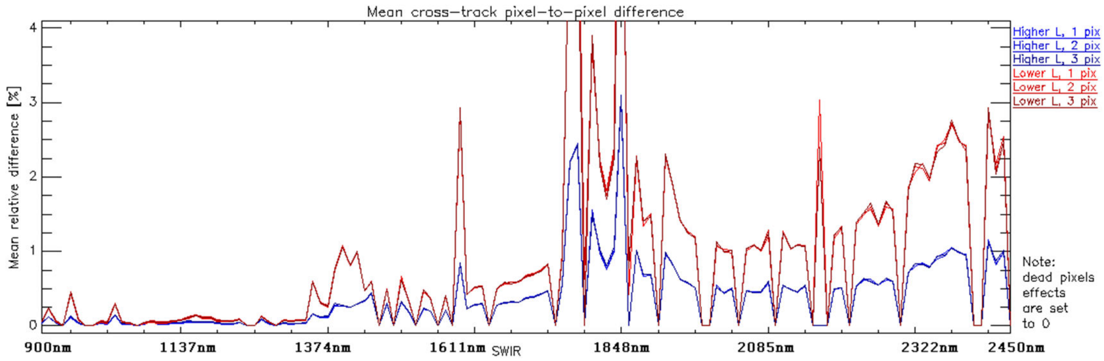

Figure 7-22 SWIR mean cross-track pixel-to-pixel difference

Another – independent – analysis estimating the magnitude of the striping effect was carried out for a subset of homogeneous desert sites using the methodology proposed for Sentinel-2 [9] as shown in Figure 7-23.

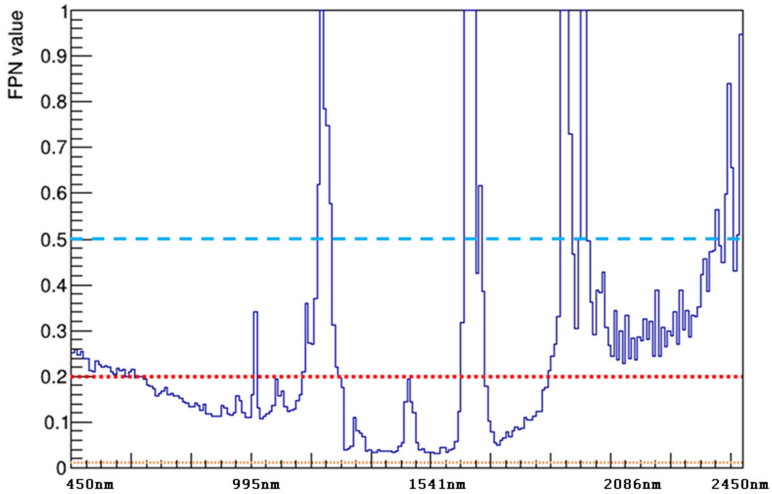

Blue line: typical EnMAP FPN values; orange line: typical Sentinel-2 FPN values; dashed blue: EnMAP RNU requirement (0.5%); dashed red: Sentinel-2 FPN requirement (0.2%)

Figure 7-23 Fixed Pattern Noise (FPN) analysis using methodology proposed for Sentinel-2

To summarize, regarding striping / fixed-pattern noise (FPN), EnMAP performs for most bands and most land observations within the response non-uniformity requirements. As the signals decrease, the impact of the additive nature of the phenomenon increases.

2. Image Artefacts: VNIR Fringing / Etaloning

Fringing (also known as etaloning) is an expected effect of the VNIR CMOS detector. Fringing is a mixed spectral and radiometric effect. The Level 1B product shows an along-track low frequency variation which is constant across all frames (see Figure 7-24 and Figure 7-25) and does not appear in the lower bands nor in the SWIR (Figure 7-26). These fluctuations also appear in the across-track profiles shown in Figure 7-27, causing a wave pattern towards the edges of the image for the VNIR bands at longer wavelengths. Note that due to the very homogeneous observation site and the stacked plots in Figure 7-27 the fringing is highlighted, and usually shows less impact on observations. Based on results from the DESIS mission which features a VNIR CMOS detector from the same waver (but with differences regarding shutter and read-out wavelengths), the stability and the magnitude of the fringing strongly depends on the observation, not allowing for a generally valid estimation of the magnitude.

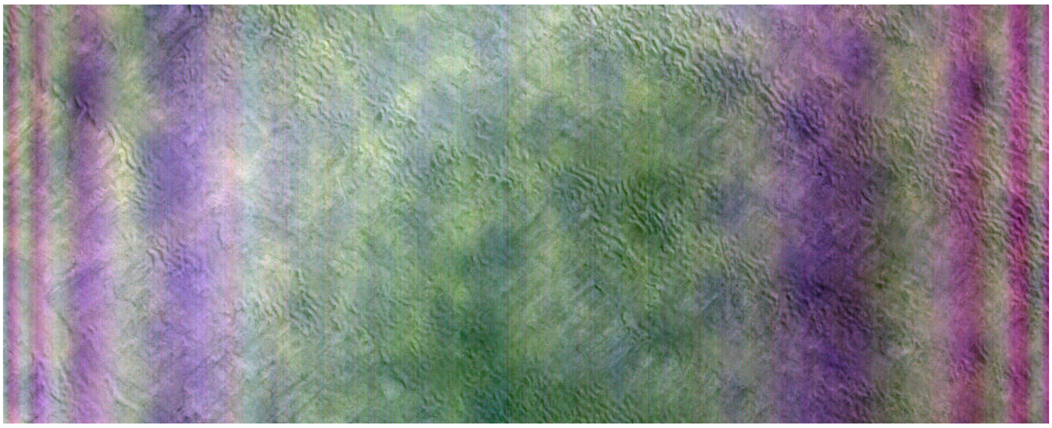

Figure 7-24 Fringing of the VNIR, illustrated by non-linear image stretch over homogeneous PICS

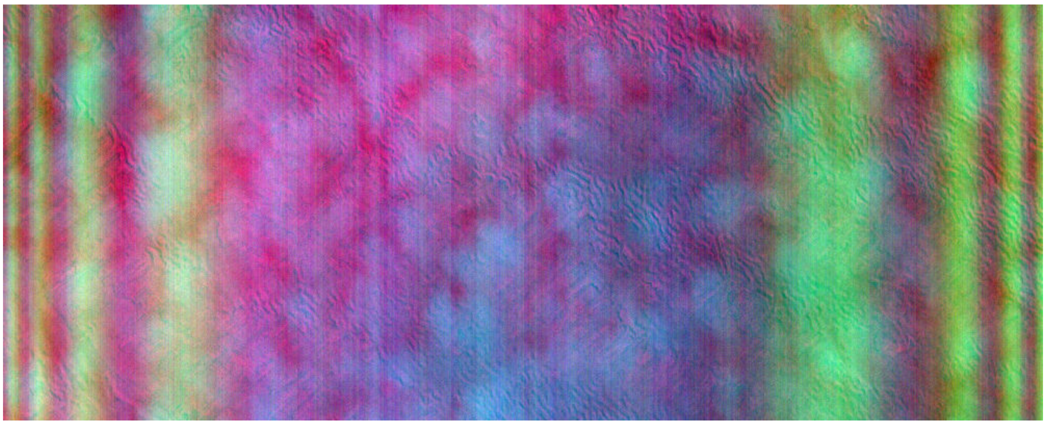

Figure 7-25 Fringing of the VNIR, Principal Component-transformed data

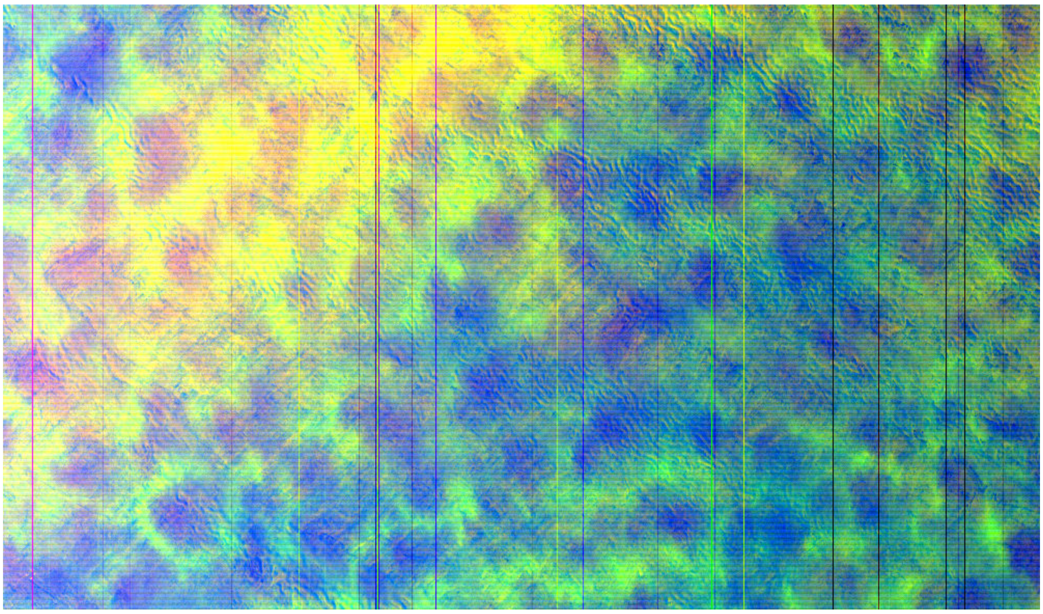

Figure 7-26 Principal Component-transformed data of the SWIR (no fringing) for comparison

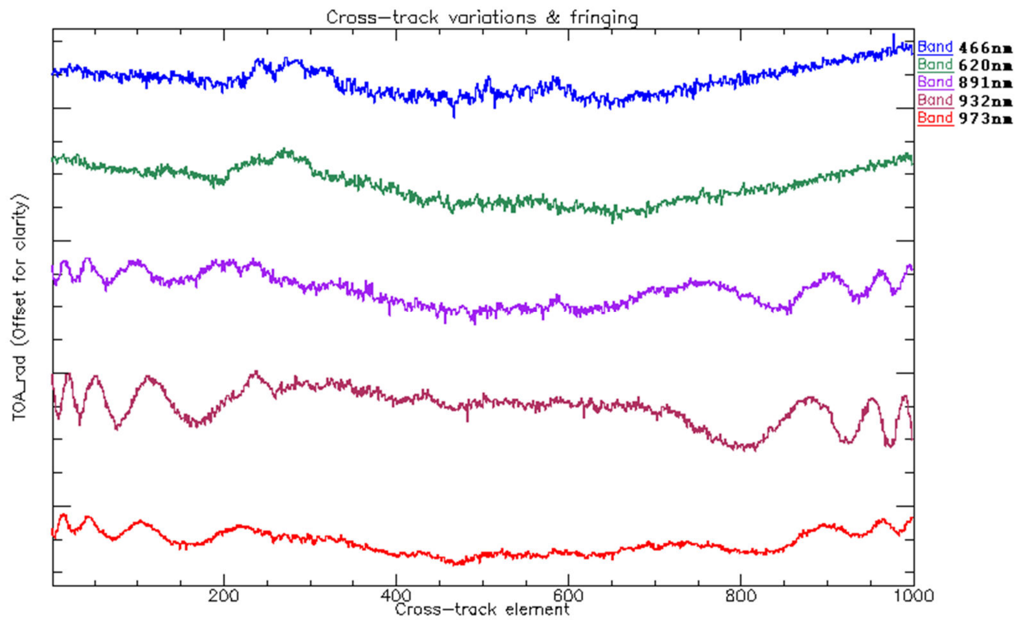

Figure 7-27 Across-track profiles for various VNIR bands, fringing influence increases towards bands at longer wavelengths

3. Image Artefacts: Micro-Vibration Effects on the SWIR

An additional effect on the SWIR is along-track striping due to SWIR-A compressor micro-vibration harmonics, resulting in a regular striping pattern in along-track direction, as highlighted by a principal component transformation shown in Figure 7-28. As shown in Figure 7-29, the magnitude of the along-track striping is relatively small and cyclic, with a relative magnitude below approx. 1% (which also includes the influence of the natural heterogeneity of the site).

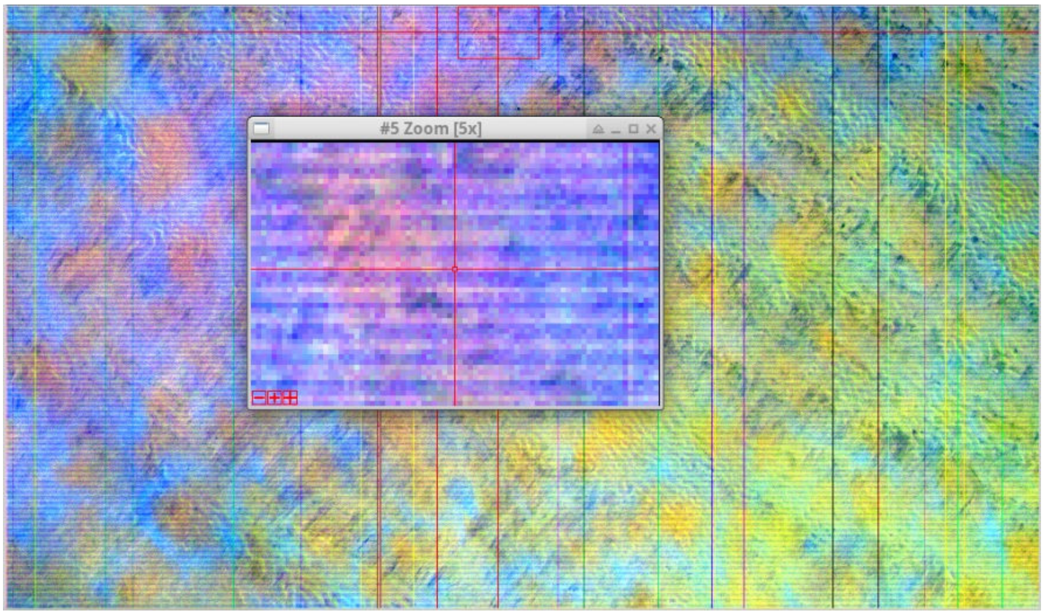

Figure 7-28 Principal Component Analysis (PCA) highlighting along-track striping

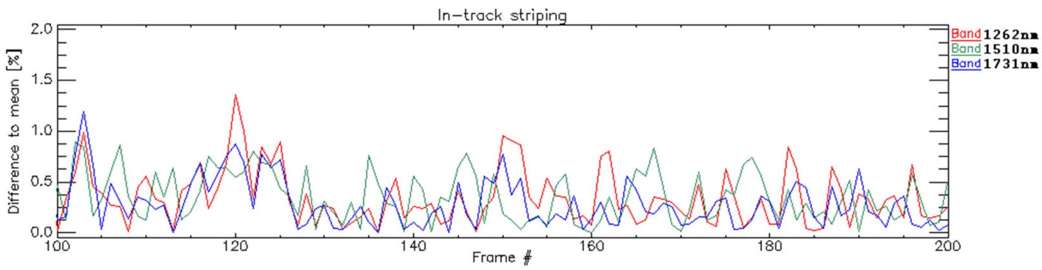

Values in [%] relative to the average.

Figure 7-29 Along-track profiles in Level 1B TOA radiances for 100 frames

- To summarize, concerning Level 1B:
    - Spectral stability and smile are within the requirements of the mission.
    - Absolute and relative radiometric calibrations are within the requirements of the mission.
    - Striping and other image artefacts are within the requirements of the mission.
- The three identified anomalies, i.e. striping and fixed pattern noise, VNIR fringing / etaloning, SWIR micro-vibration effects, and methods for their correction are under further investigation.

7.6.3 Level 1C

This report covers the timeframe between 01.10.2022 and 31.12.2022. A geometric calibration was performed end of October 2022 and the resulting calibration table is valid since 03.11.2022. Thus for the assessment of the geometric accuracy and the co-registration accuracy, only data acquired after 03.11.2022 were used, while for the statistics in this section all data acquired between 01.10.2022 and 31.12.2022 were analyzed. Due to several challenges with the satellite several outages occurred, the last data in 2022 was acquired on 12.12.2022.

In the timeframe of this report, 965 datatakes have been acquired. In 440 of those datatakes (~46%), enough GCPs and ICPs were found to perform a geometric accuracy assessment. The datatakes without enough GCPs were not assessed quantitatively, but a random subset of them was inspected visually. The vast majority of those datatakes was either almost fully covered with clouds or showing only water, desert or rain forest. The behavior is thus as expected. The assessment of the RMSE values in the metadata is shown below in Figure 7-30.

In x-direction, only 2 datatakes (~0.5%) are above 30 m (1 GSD), whereas in y-direction, 8 datatakes (~2%) are above this threshold. The mean values are 8.6 m in x-direction and 18 m in y direction. This shows a very high geolocation accuracy for the datatakes where matching was possible. The requirement of 30 m (1 GSD) is thus fulfilled.

The average boresight angles, which can be interpreted as the correction and thus the error of the scene if no GCPs could have been found, corresponds to approximately 32 m in x direction and -22 m in y direction on ground with a standard deviation of approximately 31 m and 71 m in x- and y direction respectively. It is reasonable to assume that the scenes where no GCPs could be found are in the same accuracy range and thus well within the requirement of 100 m.

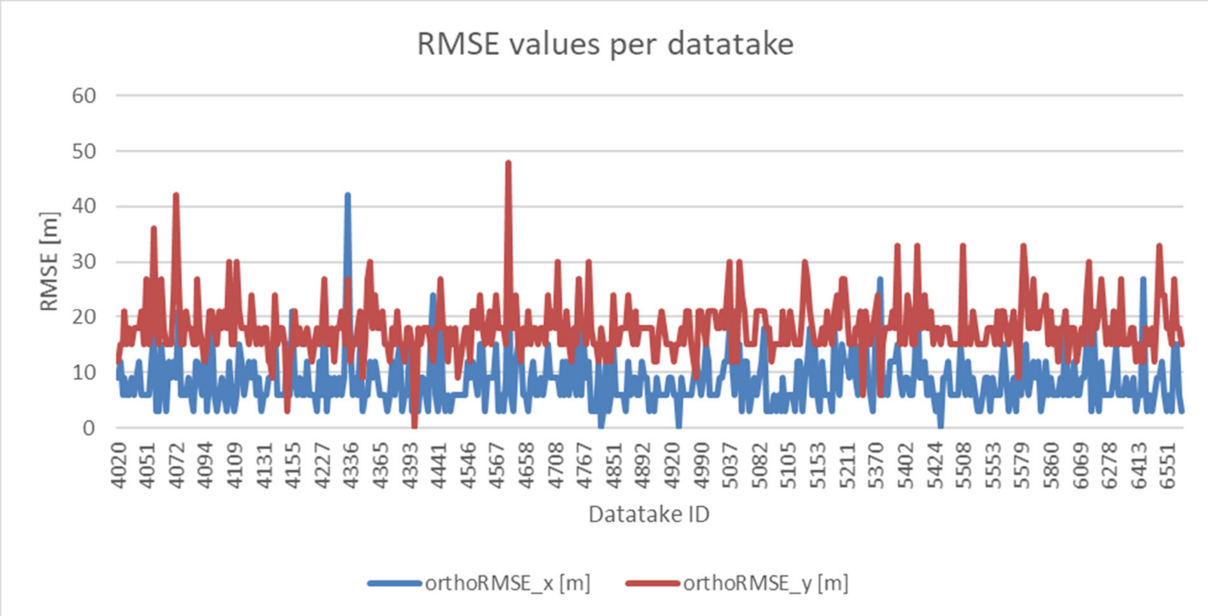

Figure 7-30 Geometric Accuracy RMSE values estimated based on identified ICPs, for all observations (x-axis: DT, y-axis: m)

7.6.3.1 Geometric accuracy

EnMAP Level 1C products are matched against a reference image (Sentinel-2 data, if not stated otherwise) by using image matching techniques to assess the geometric accuracy. At the obtained checkpoints, statistics are calculated to provide mean and RMSE values for each scene. A random sample of 105 L1C tiles was selected based on visual inspection of the catalogue quicklooks (e.g. to avoid cloudy images).

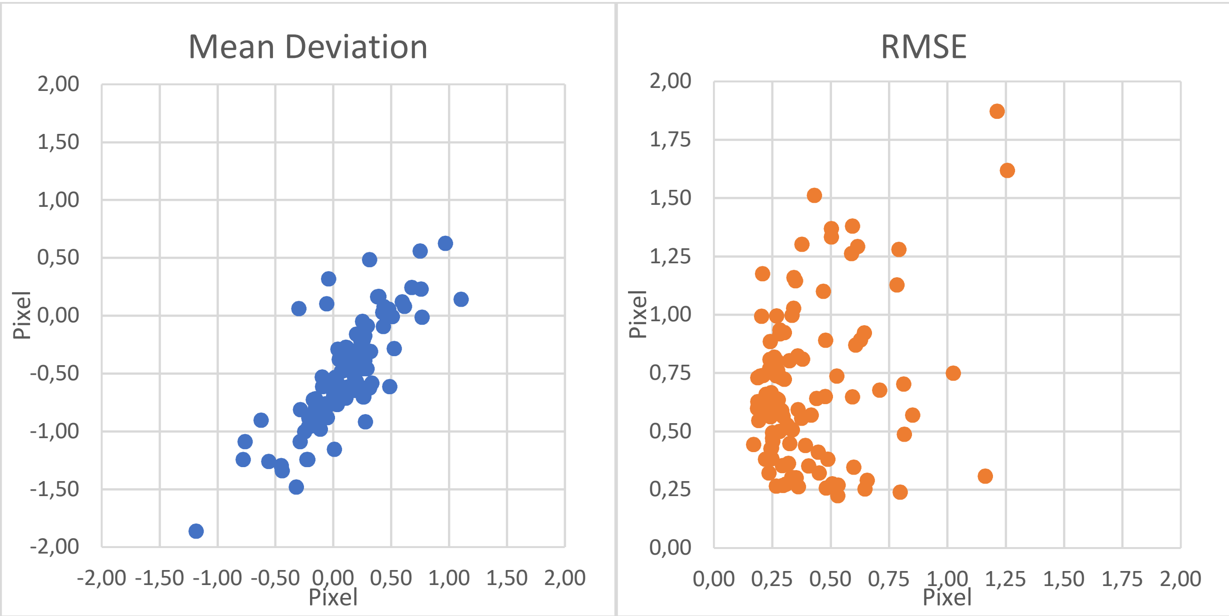

Figure 7-31 Mean deviation (left) and RMSE value (right) of Level 1C products with respect to the reference image measured in pixels

Note, that during processing the boresight angles and the geometric accuracy related quality flags are calculated on datatake-level while in the figures and tables above, the accuracy is assessed per tile. The mean values over all 105 L1C tiles are 0.11 and -0.50 pixel in mean deviation and 0.41 and 0.69 pixel for RMSE, both in x and y direction respectively. The data show, that for the vast majority of scenes the accuracy wrt reference image is better than one pixel and thus the requirements are fulfilled.

7.6.3.2 Co-registration accuracy

For the assessment of co-registration accuracy, the SWIR data of EnMAP Level 1C products are matched against the corresponding VNIR data.

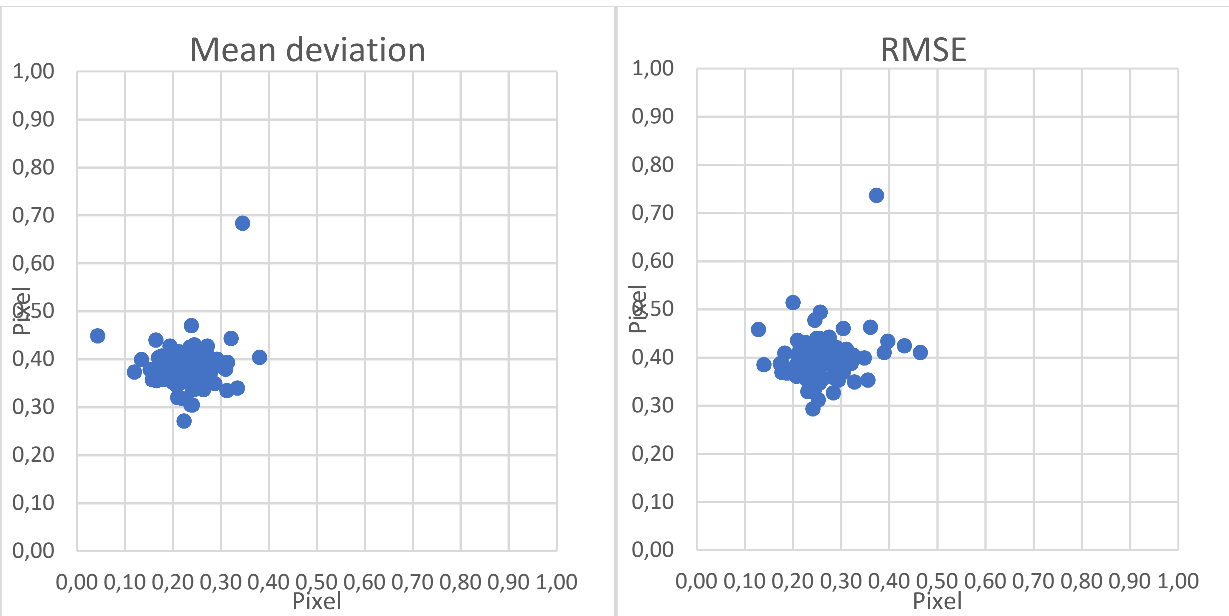

Figure 7-32 Mean deviation (left) and RMSE value (right) of the difference between VNIR and SWIR image on Level 1C products measured in pixels

The data show, that the co-registration is in the order of 0.2 pixel in x-direction and 0.4 pixel in y-direction. This is still slightly above the requirement. Note that the x- and y-direction are not in the image coordinate system but in UTM, as the evaluation is done on L1C products. When looking at the direction of the offset, it is mainly in flight direction. Based on these findings, we are currently working on a further improvement of the co-registration accuracy and are very confident that we can achieve this with the next update of the geometric calibration table.

7.6.4 **Level 2A**

Within the time interval between 01.10.2022 and 31.12.2022, an interactive in-depth analysis has been conducted for the following scene:

Reference	Datatake ID	L2A Processing Version	Comment
[L2A-1]	DT0000004713_20221022T045622Z_002	01.01.11	Nominal quality (overall quality=0)

The quality of the Level 2A data was examined using this scene as an example. A consistency check between L2A and ATCOR results did not show any anomalies. Visible differences (e.g. due to different aerosol or water vapor) are within the expected range:

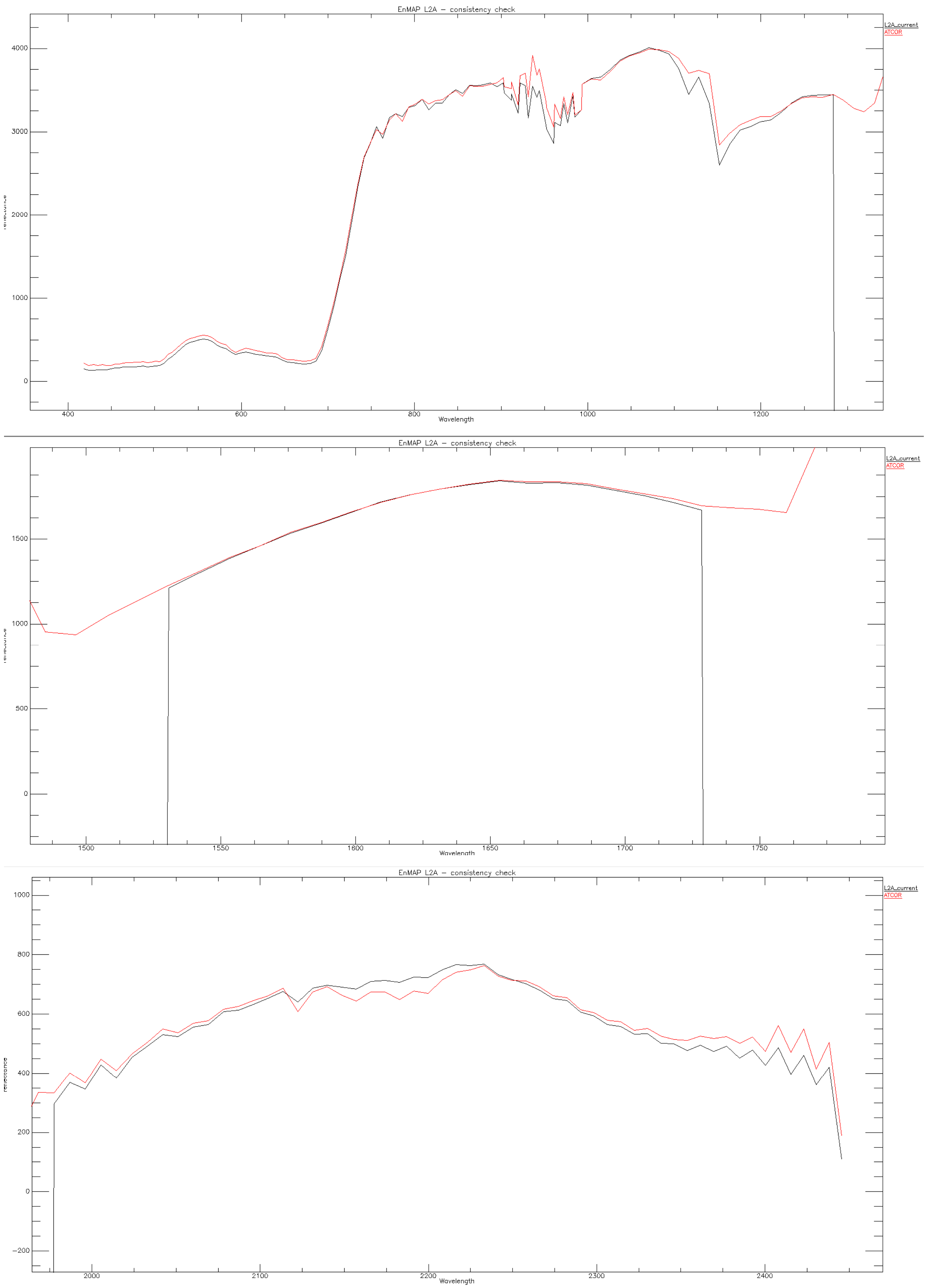

Figure 7-33 Mean spectra over land (400x400 pixel) of Level 2A (black) and ATCOR (red) results

The L2A product shows the “combined” version, i.e. PACO results over land, and MIP results over water. There is a visible boundary effect between land and water pixels e.g. at the river bank. It looks like defective pixels, but is in fact a feature of the combined mode, and therefore consistent with the specifications.

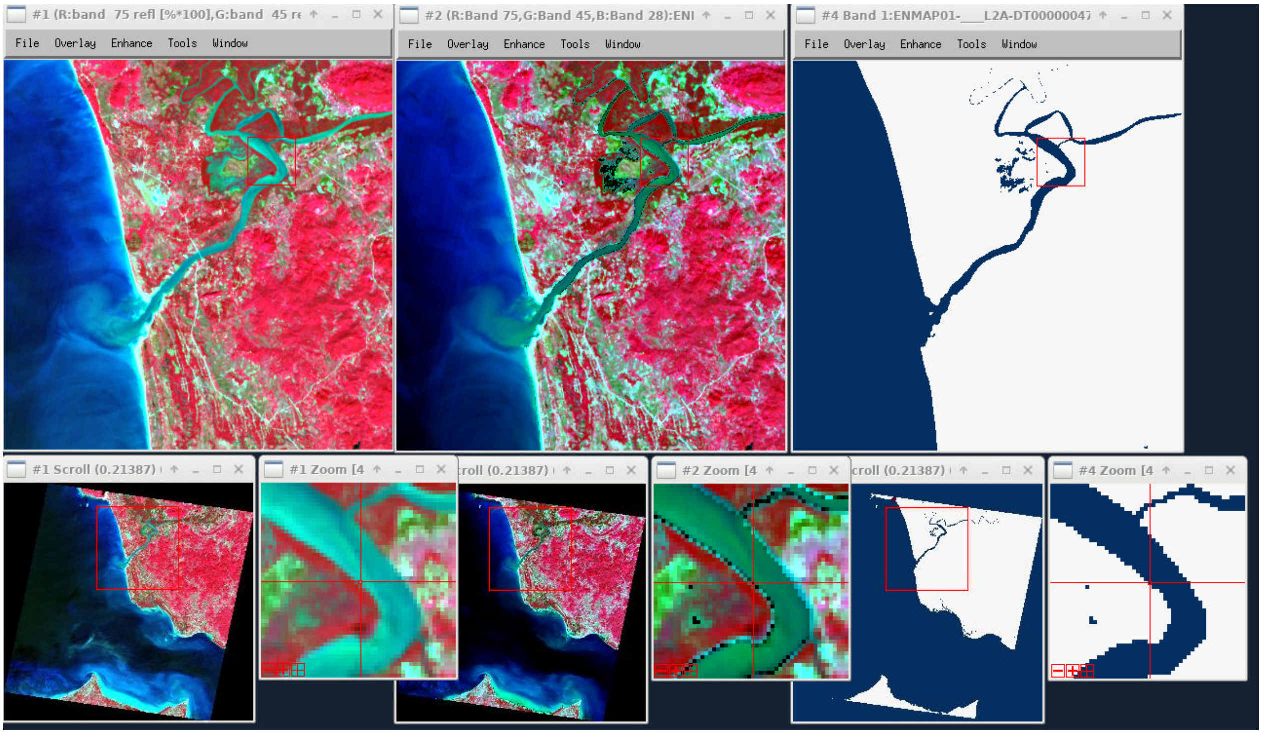

Left: ATCOR results (no differentiation between land and water), middle: Level 2A results (combined version with MIP processing used for water pixels and PACO processing for land pixels); right: land-water classification results

Figure 7-34 Visible boundary effects between land and water

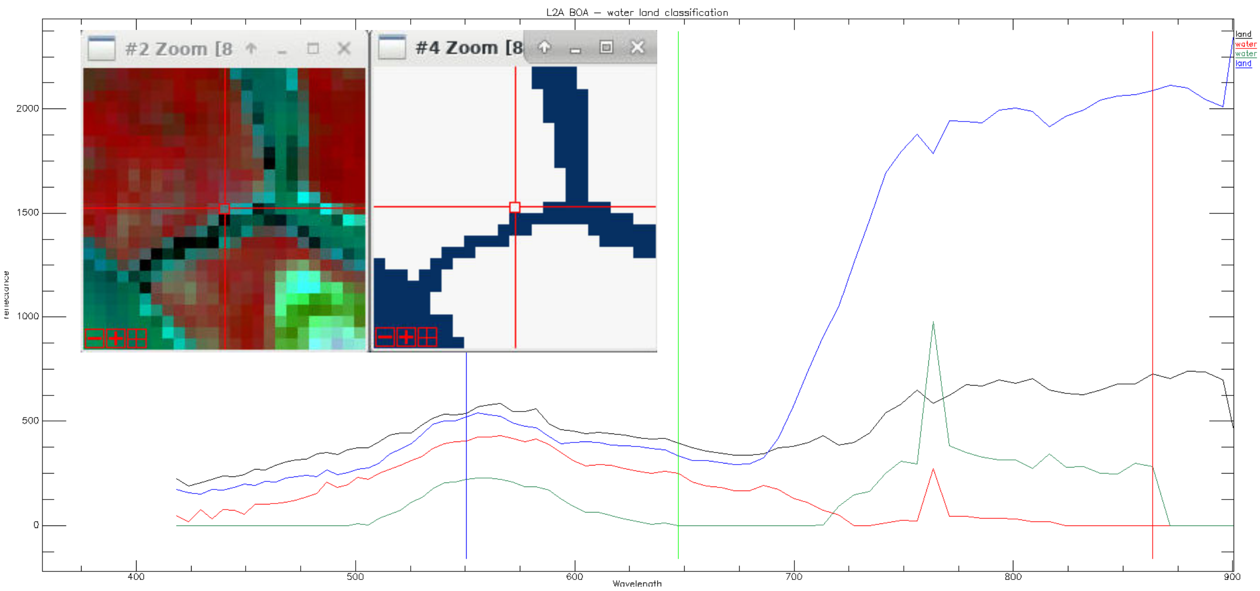

Red/green = water pixels (value set to zero at NIR); black/blue = land pixels

Figure 7-35 Single pixel spectra of Level 2A at the river

8. External Product Validation

In the reporting period, the focus of the external product validation was on the VNIR-to-SWIR spatial co-registration as well as on the statistical assessment of the L2A water leaving reflectance. For both validations, minor anomalies were indicated during the commissioning phase.

8.1.1 Level 1B

Level 1B products were not validated in detail and in-depth during the reporting period. Level 1B products have been validated regarding

- Signal-to-Noise Ratio (SNR)
- Spatially coherent radiometric miscalibration (striping artifacts)

The documented SNR requirements (which referred to an SSD of 10 nm and 30% reflective target) were adopted to the actual EnMAP SSD: VNIR > 343:1 (@495 nm & SSD 4.7 nm) and SWIR > 137:1 (@2200 nm & SSD 8.4 nm) for L(TOA) reference of 30% reflective target. After this adaptation of the SNR mission requirements, the signal-to-noise ratio (SNR) was estimated for the VNIR and SWIR sensors based on 62 regular earth data takes. The estimations can be taken as the minimum SNR and the results give a realistic indication of the existing SNR for the user. The SNR at 495 nm reaches 296:1 for the earth data takes. This results in an SNR reference equivalent of ~354:1. Thus the SNR requirement VNIR > 343:1 (@495 nm & SSD 4.7 & 30% reflective target) is fulfilled. The SNR at 2200nm reaches 294:1 for the analyzed data takes. This results in an SNR reference equivalent of ~260:1. Thus the SNR requirement SWIR > 137:1 (@2200 nm & SSD 8.4 & 30% reflective target) is fulfilled.

The spatially-coherent radiometric striping artifacts and undulations in the VNIR and SWIR across-track direction have been validated again. No improvement could be observed. The same applies to the along-track artifacts detected in SWIR wavelength domains with a strong gradient/feature. Although the radiometric mis-registrations are very small and thus far below the requirements of < 5 %, a correction should be integrated in the future since the artifacts influence the thematic products of the user and the quantitative determination.

8.1.2 Level 1C

Level 1C products have been validated regarding:

- VNIR-to-SWIR spatial co-registration
- Absolute spatial accuracy

The relative geometric accuracy between the VNIR and SWIR was validated based on 58 tiles. Spatially variable shifts between the spectrally overlapping VNIR band 95 and the SWIR band 96 were derived. An aggregated relative spatial accuracy statistic was generated, including validation results of 44 tiles acquired before 03.11.2022 and of 14 tiles acquired after 03.11.2022 by default processed with the current geometric calibration. For acquisitions acquired before 03.11.2022 (44 tiles), the RMSE in the x-direction (22.92 m) and y-direction (19.84 m) does not meet the mission requirements (< 30 % of a pixel) due to the lack of valid geometric calibration during this period. For the tiles acquired after 03.11.2022 a valid geometric calibration is in use and the RMSE in the x-direction (7.74 m) and y-direction (11.91 m) comes very close to the requirements of the mission of < 30 % of a pixel.

The absolute spatial accuracy validation statistic based on 36 tiles indicates that the mission requirements are fulfilled. The RMSE in the x-direction (23.09 m) and y-direction (21.59 m) are both inside the mission requirements of 30 m (1 GSD).

8.1.3 Level 2A

During the reporting period, only L2A water products have been validated based on match-ups of in-situ and EnMAP earth observations.

Water

The validation of L2A normalized water leaving reflectance was conducted at four study sites: the Lucinda Jetty Coastal Observatory (LJCO) in the Great Barrier Reef, the Aqua Alta Oceanographic Tower (AAOT) in the Gulf of Venice, Lake Constance, and Lake Trasimeno. The statistical analysis of the product validation indicates that the requirements were mostly met. In general, the match-ups demonstrated a slight underestimation of the EnMAP level 2 normalized water leaving reflectance product compared to in situ measurements. The calculated uncertainties (RMSE) were confronted with the mission requirements for L2A normalized water leaving reflectance (AOT at 550 nm < 0.4 is: 0.04 for 400 nm < $\lambda \leq$ 450 nm, 0.02 for 450 nm < $\lambda \leq$ 650 nm and 0.01 for 450 nm < $\lambda \leq$ 800 nm. For AOT at 550 nm > 0.4 the corresponding requirement increase by 0.01). The requirements were met for 6 out of 7 match-ups in the visible range, although uncertainties were larger in the 400-550 nm wavelength domain. The EnMAP spectrum showed systematic peaks and valleys at various wavelengths (e.g. at 429.29, 434.53, 449.39, 486.94, and 501.09 nm), with higher magnitudes observed at AAOT. The causes of these peaks and valleys require further investigation. To improve the quality of the EnMAP level 2 normalized water leaving reflectance product, more coincident EnMAP and in situ measurements are needed.

8.1.4 Summary of External Product Validation

The focus during the reporting period was on validations where minor non-compliances with the mission requirements were indicated during the commissioning phase. Namely the insufficient geometric VNIR-to-SWIR co-registration and the L2A normalized water leaving reflectance product. Both validation scenarios are now very close (VNIR-to-SWIR co-registration) and inside (L2A normalized water leaving reflectance) the mission requirements. There were no improvements regarding the across-track stripe pattern. However, these are expected in the next reporting period.

9. Others

During the reporting period the EnMAP mission was presented at many international conferences, e.g.

- Waterdays - SBD and EO Technology Conference, Herrsching, Germany (04.10.2022-06.10.2022)
- 2nd Workshop on International Cooperation in Spaceborne Imaging Spectroscopy, Frascati, Italy (19.10.2022-21.10.2022)